Clim. Past Discuss., 5, 1553–1607, 2009
www.clim-past-discuss.net/5/1553/2009/
© Author(s) 2009. This work is distributed under
the Creative Commons Attribution 3.0 License.

Climate of the Past Discussions

Climate of the Past Discussions is the access reviewed discussion forum of *Climate of the Past*

Variations in mid-latitude North Atlantic surface water properties during the mid-Brunhes: Does Marine Isotope Stage 11 stand out?

A. H. L. Voelker[1,2], T. Rodrigues[1], R. Stein[3], J. Hefter[3], K. Billups[4], D. Oppo[5], J. McManus[5,*], and J. O. Grimalt[6]

[1]Dept. Geologia Marinha, Laboratorio Nacional de Energia e Geologia (LNEG; ex-INETI), Estrada da Portela, Zambujal, 2721-866 Alfragide, Portugal
[2]CIMAR Associate Laboratory, Rua dos Bragas 289, 4050–123 Porto, Portugal
[3]Alfred-Wegener-Institute for Polar and Marine Research, Columbusstrasse, 27568 Bremerhaven, Germany
[4]College of Marine and Earth Studies, University of Delaware, 700 Pilottown Road, Lewes, DE 19958, USA

[5]Geology and Geophysics, Woods Hole Oceanographic Inst., Woods Hole, MA 02543, USA
[6]Department of Environmental Chemistry, Institute of Chemical and Environmental Research (CSIC), Jordi Girona 18, 08034-Barcelona, Spain
*now at: Department of Earth and Environmental Science, Columbia University, Lamont-Doherty Earth Observatory, 61 Route 9W, Palisades, NY 10964–8000, USA

Received: 16 May 2009 – Accepted: 20 May 2009 – Published: 3 June 2009

Correspondence to: A. Voelker (avoelker@softhome.net)

Published by Copernicus Publications on behalf of the European Geosciences Union.

Abstract

New planktonic stable isotope and ice-rafted debris records from three core sites in the mid-latitude North Atlantic (IODP Site U1313, MD01-2446, MD03-2699) are combined with records of ODP Sites 1056/1058 and 980 to reconstruct hydrographic conditions during the middle Pleistocene spanning Marine Isotope Stages (MIS) 9–14 (300–540 ka). Together the study sites reflect western and eastern basin boundary currents as well as north to south transect sampling of subpolar and transitional water masses. Planktonic $\delta^{18}O$ records indicate that during peak interglacial MIS 9 and 11 hydrographic conditions were similar among all the sites with relative stable conditions and confirm prolonged warmth during MIS 11c also for the mid-latitudes. Sea surface temperature (SST) reconstructions further reveal that in the mid-latitude North Atlantic MIS 11c is associated with two plateaus, the younger one of which is slightly warmer. Enhanced subsurface northward heat flux in the eastern boundary current system, especially during early MIS 11c, is denoted by the presence of tropical planktonic foraminifer species. MIS 13 was generally colder and more variable than the younger interglacials. The greatest differences between the sites existed during the glacial inceptions and glacials. Then a north-south trending hydrographic front separated the nearshore and offshore waters off Portugal. While offshore waters originated from the North Atlantic Drift as indicated by the similarities between the records of IODP Site U1313, ODP Site 980 and MD01-2446, nearshore waters as recorded in core MD03-2699 derived from the Azores Current and thus the subtropical gyre. A strong Azores Current influence is seen especially during MIS 12, when SST dropped significantly only during the Heinrich-type ice-rafting event at the onset of Termination V. Given the subtropical overprint on Portuguese nearshore sites such as MD03-2699 and MD01-2443 caution needs to be taken to interpret their records as basin-wide climate signals.

CPD

5, 1553–1607, 2009

1 Introduction

The Brunhes polarity chron encompasses the last 780 ka (kiloannum = thousand year) and its middle section is often considered as a particularly warm period during the last 1000 ka, when warm surface waters penetrated polewards and sea levels were generally higher than at Present (Droxler et al., 2003). MIS 11 and 9 are part of this warm interval. Interglacial MIS 11c was the first interglacial period after the mid-Pleistocene transition with atmospheric greenhouse gas concentrations and temperatures over Antarctica (Petit et al., 1999; Siegenthaler et al., 2005; Spahni et al., 2005; Jouzel et al., 2007) at levels similar to those during subsequent interglacials including the current one, the Holocene. Based on temperature related proxy records from the oceans (Hodell et al., 2000; Lea et al., 2003; McManus et al., 2003; de Abreu et al., 2005; Helmke et al., 2008) and from Antarctica (Petit et al., 1999; Jouzel et al., 2007) it was an unusually long lasting interglacial and northern heat piracy, i.e. the enhanced advection of warm waters from the South into the North Atlantic, was at its maximum (Berger and Wefer, 2003). The early temperature rise during the high amplitude transition from glacial MIS 12 to MIS 11c leads to two possible definitions for the duration of the interglacial period within MIS 11. Based on the interval of maximum warmth in marine records, the interglacial period lasted at minimum from to 420 to 396 ka (McManus et al., 2003; Helmke et al., 2008). The definition of an interglacial as the period of ice volume minimum/sea-level highstand (Shackleton, 1969), however, shortens this interval to 409 to 396 ka (based on the LR04 chronology; Lisiecki and Raymo, 2005). This shorter period is also the interval, when full interglacial conditions, including minimal ice-rafting, occurred in the Nordic Seas (Bauch et al., 2000). Because of the similarity in the eccentricity signal (Loutre and Berger, 2003), MIS 11c is the interglacial often used as equivalent to the Holocene. In the subpolar North Atlantic at ODP Site 980 the peak interglacial period, MIS 11c, is recorded as a long, stable interval with relatively small SST variations (Oppo et al., 1998; McManus et al., 2003), while the later phase of MIS 11, contemporary with the built-up of continental ice sheets during the

CPD
5, 1553–1607, 2009

inception of glacial MIS 10, is marked by millennial-scale variability linked to ice-rafting events and southward incursions of arctic surface waters (Oppo et al., 1998; McManus et al., 1999). On the western boundary of the subtropical gyre at ODP Site 1056, on the other hand, peak interglacial conditions were more variable in the surface water as evidenced by short-term incursions of colder surface waters, while thermocline conditions were relative stable and comparable to the Holocene (Chaisson et al., 2002; Billups et al., 2004). During the transition to MIS 10 the Gulf Stream waters at ODP Site 1056 experienced higher temperature variability linked to cooling episodes in the surface and thermocline waters (Chaisson et al., 2002; Billups et al., 2004), episodes that are contemporary with those recorded at ODP Site 980.

The interglacial after MIS 11c was MIS 9e – following (Tzedakis et al., 1997) we are dividing MIS 9 into five substages instead of three (Bassinot et al., 1994). MIS 9e is a better analog for the Holocene than MIS 11c if tilt and insolation are emphasized for the comparison (Ruddiman, 2006). During MIS 9e ice volume minimum and temperature maximum coincided e.g. (McManus et al., 1999; Martrat et al., 2007) with the sea-level highstand being dated approximately to 334 to 306 ka (Stirling et al., 2001). In the Antarctic ice core records, MIS 9e is marked by an early maximum in temperature (Petit et al., 1999; Watanabe et al., 2003; Jouzel et al., 2007) and greenhouse gas concentrations (Petit et al., 1999; Loulergue et al., 2008), when values even exceeded pre-industrial Holocene levels. Such an overshooting is, however, not seen in high-resolution marine or terrestrial records from the northern hemisphere (McManus et al., 1999; Prokopenko et al., 2002; Tzedakis et al., 2004; Martrat et al., 2007; Desprat et al., 2009; Tzedakis et al., 2009).

As mentioned above, MIS 11c marked a transition in interglacial conditions, the so called mid-Brunhes event (Jansen et al., 1986). Mid-Pleistocene interglacials prior to MIS 11c were colder in Antarctica (EPICA Members, 2004) and had lower carbon dioxide concentrations (Siegenthaler et al., 2005; Lüthi et al., 2008). The LR04 benthic stack (Lisiecki and Raymo, 2005) clearly reveals that ice volume was larger during MIS 13 than during MIS 11 or 9. In terrestrial records from Tenaghi Philippon (Tzedakis

et al., 2006), Lake Baikal (Prokopenko et al., 2002) or the Chinese Loess Plateau (Guo et al., 2000), on the other hand, MIS 13 does not differ greatly from some of the subsequent interglacials, especially MIS 11. Besides these differences in climatic responses on land and in the ocean, MIS 13 is unique in the timing of full interglacial conditions. Maximum warmth and ice volume minimum of all the other interglacials during the last 700 ka occurred during the first substage after the Termination, i.e. after the transition from a glacial maximum to the interglacial sea-level highstand. During MIS 13, however, the interval of ice volume minimum (Lisiecki and Raymo, 2005) and maximum warmth in the EDC ice core record (Jouzel et al., 2007) coincided not with the first, but with the third substage, MIS 13a. Thus we regard MIS 13a as the full interglacial interval within MIS 13, even if atmospheric carbon dioxide concentrations were at a similar level during both warm substages, MIS 13c and 13a (Siegenthaler et al., 2005), and nitrous dioxide peaked during MIS 13c (Spahni et al., 2005).

One of the reasons why MIS 13 is so different, might be that its preceding glacial, MIS 14, was so weak with sea level lowering only about as half as during MIS 16, 12 or 10. Consequently, also the amplitude of Termination VI was much lower than during Terminations V or IV. MIS 12, on the other hand, was one of the most extreme glacials during the last 1000 ka, when sea level was probably lower than during the last glacial maximum (MIS 2) (Lisiecki and Raymo, 2005). Sea level during MIS 10 was similar to MIS 2, even though MIS 10 lasted only half as long as MIS 12. In regard to dust flux in Antarctica MIS 14 is also the weakest and MIS 12 the strongest glacial (Lambert et al., 2008). This pronounced difference between the mid-Brunhes glacials is, however, not evident in the EDC temperature and greenhouse gas records (Jouzel et al., 2007; Loulergue et al., 2008; Lüthi et al., 2008). Greenhouse gas concentrations during the MIS 10 glacial maximum were actually lower than during MIS 12 and 14.

One of the most prominent features of the last glacial inception is the periodic occurrence of major ice-rafting events, the so called Heinrich events (e.g. Hemming, 2004). During the Brunhes chron Heinrich-type ice-rafting events were first observed at the end of MIS 16 (Hodell et al., 2008) and then more regularly within MIS 12 and 10 (Mc-

Manus et al., 1999; Hodell et al., 2008; Ji et al., 2009). McManus et al. (1999) showed that the onset of millennial-scale climate variability, including ice-rafting events, is linked to a threshold value of 3.5‰ in benthic $\delta^{18}O$. As soon as this ice volume threshold was passed the Atlantic meridional overturning circulation (AMOC) became less stable resulting in oscillations between weaker and stronger AMOC modes. Most of the existing evidence for millennial-scale AMOC variability during the mid-Brunhes and its impacts on surface and deep waters is linked to the inception of MIS 10 (Poli et al., 2000; Billups et al., 2004; de Abreu et al., 2005; Hall and Becker, 2007; Martrat et al., 2007; Dickson et al., 2008; Stein et al., 2009). Only records from ODP Sites 980 and 1058 cover the older glacials with sufficient resolution (McManus et al., 1999; Flower et al., 2000; Billups et al., 2006; Weirauch et al., 2008) and here we present the previously unpublished planktonic $\delta^{13}C$ records for these sites.

The new records fill the gap between ODP Sites 1056 and 980 and reveal, if hydrographic conditions in the mid-latitude North Atlantic, which encompasses the southern edge of the North Atlantic ice-rafted debris (IRD) belt (Ruddiman, 1977; Hemming, 2004) and experienced large SST gradients during glacials (Calvo et al., 2001; Pflaumann et al., 2003) and stadials (Chapman and Maslin, 1999; Oppo et al., 2001), were more similar to those in the subtropical or the subpolar gyre during interglacials, especially during MIS 11. The two new records off Portugal, MD01-2446 and MD03-2699, furthermore, allow for the first time to reconstruct and evaluate the full transition from glacial MIS 12 to MIS 11 in this eastern boundary upwelling system. By combining the planktonic foraminifer stable isotope records from three new sites in the mid-latitude North Atlantic Ocean with those from ODP Sites 980 and 1056/1058 we aim (1) to map hydrographic conditions within the major surface currents (Fig. 1) and thus to identify potential latitudinal or longitudinal gradients in the North Atlantic during the interval spanning from MIS 9c to 14 (300–540 ka); (2) to trace the potential sources of the subsurface waters and their changes on glacial and interglacial timescales; and (3) to address the question, how stable or variable hydrographic conditions were in the mid-latitude North Atlantic during MIS 11 and how they differed from those during its

CC BY

neighboring interglacials, MIS 13 and 9. Our interpretation is supported by IRD records for the three new sites and for alkenone-based SST data for MIS 11 from two of those sites.

2 Core sites and modern hydrographic setting

The three new core sites are IODP Site U1313, MD01-2446 and MD03-2699 (Table 1; Fig. 1). IODP Site U1313, which re-occupies the position of DSDP Site 607, was drilled in 2005 with R/V Joides Resolution during International Ocean Drilling Program (IODP) Expedition 306 (Channell et al., 2006). Calypso piston cores MD01-2446 and MD03-2699 were retrieved with R/V Marion Dufresne during the Geosciences cruise in 2001 and the PICABIA cruise in 2003, respectively. For tracing central/mode water masses within in the North Atlantic we combine the new records with those of ODP Site 980 in the subpolar North Atlantic and of ODP Sites 1056 and 1058 from the western subtropical gyre (Table 1; Fig. 1a).

Surface waters at all sites are derived in one form or another from the Gulf Stream and the North Atlantic Current (NAC). ODP Sites 1056 and 1058 are located directly below the Gulf Stream, while ODP Site 980 is influenced by the Rockall Trough branch of the NAC (Fratantoni, 2001; Brambilla and Talley, 2008). Even though IODP Site U1313 is located south of the core NAC pathway, drifter data shows that surface waters in this area are derived from the NAC, partly through recirculation off the Grand Banks (Fratantoni, 2001; Reverdin et al., 2003).

Gulf Stream/NAC derived surface waters off the western Iberian Peninsula are transported by two currents, the Portugal Current and the Azores Current. The Portugal Current (PC) is the NAC recirculation branch within the northeastern North Atlantic (Fig. 2a) and is centered west of 10° W off Portugal (Peliz et al., 2005). Thus it is the current influencing site MD01-2446 (Fig. 1b). The PC advects freshly ventilated surface and subsurface waters slowly southward. The subsurface component of the PC is subpolar Eastern North Atlantic Central Water (ENACW) that is formed by winter

CC BY

cooling in the eastern North Atlantic (McCartney and Talley, 1982), including along the NAC's Rockall Trough branch (Brambilla and Talley, 2008). The Azores Current (AzC) diverges from the Gulf Stream and moves in large meanders between 35 and 37° N across the North Atlantic. Its northern boundary forms the subtropical Azores front. In the eastern basin the AzC splits into several branches, one of which is the Canary Current, its major recirculation, and another, the eastern branch, enters into the Gulf of Cadiz (Fig. 1). During winter, waters from this eastern branch recirculate northward as the Iberian Poleward Current (IPC) (Peliz et al., 2005), thereby bending the subtropical front northward along the western Iberian margin (Fig. 1b). Similar to the PC, the IPC includes a subsurface component: ENACW of subtropical origin. Subtropical ENACW is formed by strong evaporation and winter cooling along the Azores front (Rios et al., 1992) and is less ventilated, warmer and saltier than its subpolar counterpart (van Aken, 2001). IPC waters influence site MD03-2699, especially during fall and winter. During spring and summer (mainly May to September), on the other hand, the upwelling filaments that form off Peniche and Cape Roca can reach as far offshore as site MD03-2699, so that either upwelled waters or the seasonal, nearshore branch of the PC (Fiúza, 1984; Alvarez-Salgado et al., 2003) affect the site. Subtropical ENACW is generally upwelled south of 40° N and subpolar one north of 45° N. In between either water mass can be upwelled depending on the strength of the wind forcing. Strong winds can cause subpolar ENACW to be upwelled also south of 40° N.

Outside of the western Iberian upwelling zone plankton blooms drive surface water productivity (Table 1). Site MD01-2446 falls within the mid-latitude regime of (Levy et al., 2005) that is associated with a bloom that starts in fall and peaks in spring. The northern boundary of this regime is at 40±2° N, so that IODP Site U1313 either follows this regime or experiences a major late spring bloom and a smaller fall bloom like it is typical for the subpolar regime and for ODP Site 980. ODP Sites 1056 and 1058, on the other hand, follow the subtropical regime with a weak fall bloom.

CC BY

3 Methods

Sediment samples for stable isotope and lithics analyses of IODP Site U1313 and cores MD03-2699 and MD01-2446 were prepared in LNEG's Laboratorio de Geologia Marinha following the established procedure. After freeze drying samples were washed with deionized water through a 63 μm-mesh and the coarse fraction residue was dried in filter paper at 40°C and weighted. Sample intervals are 1–3 cm for core MD03-2699 and 2–3 cm for core MD01-2446. IODP Site U1313 was sampled continuously with 2 cm-wide scoops. Site U1313 stable isotope samples were taken from the secondary splice (Voelker et al., 2009) and biomarker samples from the primary splice (Stein et al., 2009).

For planktonic stable isotope measurements in cores MD03-2699 and MD01-2446 and IODP Site U1313, 8–10 clean specimens of *Globorotalia inflata* were picked from the fraction >315 μm. *G. inflata* is one of the dominant species in the planktonic foraminifer fauna associated with the NAC (Ottens, 1991). Its stable isotope values reflect hydrographic conditions at the base of the seasonal thermocline (Cléroux et al., 2007); conditions that are close to those in the winter mixed layer. Details on stable isotope measurements for ODP Site 980 are given by Oppo et al. (1998) and McManus et al. (1999), for ODP Site 1056 by Chaisson et al. (2002) and Billups et al. (2004) and for ODP Site 1058 by Billups et al. (2006). Because of laboratory offsets ODP Site 1056 *N. dutertrei* δ^{18}O values needed to be adjusted by +0.2‰ in order to match absolute values of ODP Site 1058.

Benthic isotope records of cores MD03-2699 and MD01-2446 and IODP Site U1313, here just used to establish chronostratigraphies, are based on 2–4 lean specimens of *Cibicidoides wuellerstorfi*, *Cibicidoides mundulus* or *Cibicidoides pachyderma* (the last only in MD03-2699). At few levels where *C. wuellerstorfi* was absent *Uvigerina* sp. was picked instead. All *Cibicidoides* sp. δ^{18}O data is corrected by +0.64‰ to the *Uvigerina* sp. level (Shackleton, 1974). Benthic and planktonic stable isotope samples were measured in a Finnigan MAT 252 mass spectrometer at Marum (University Bremen,

Germany). The mass spectrometer is coupled to an automated Kiel carbonate preparation system and the long-term precision is ±0.07‰ for $\delta^{18}O$ and ±0.05‰ for $\delta^{13}C$ based on repeated analyses of internal and external (NBS-19) carbonate standards.

The number of lithic fragments was determined in the fraction >315 μm and is presented as "#/g" (normalized by the respective sample's dry weight). Lithics are primarily interpreted as IRD. The coarser size fraction was chosen 1) to minimize modification of the IRD signal by wind deposition and lateral advection at slope site MD03-2699 and 2) to avoid scientific overlap for Site U1313 within the science party of IODP Exp. 306. Using a coarser size fraction allows to identify all the ice-rafting events (e.g. Voelker, 1999) and only this is relevant for the current study, but might underestimate the absolute intensity of an ice-rafting event.

Biomarker samples of IODP Site U1313 and core MD03-2699 were prepared following established procedures (Villanueva et al., 1997; Calvo et al., 2003). Core MD03-2699 samples were analysed in a Varian gas chromatograph either at the Dept. of Environmental Chemistry of CSIC (Barcelona) or at the Dept. de Geologia Marinha of LNEG (Rodrigues et al., 2009). Site U1313 samples were measured in a gas chromatograph/time-of-flight mass spectrometer at the Alfred-Wegner Institute, Bremerhaven (Hefter, 2008; Stein et al., 2009). Alkenone-based sea surface temperatures (SST) for both sites were calculated using the unsaturation index $U_k^{37'}$ of Müller et al. (1998) and thus should reflect annual mean SST.

IODP Site U1313, MD01-2446 and MD03-2699 data will be stored at the World Data Centre Mare (http://www.wdc-mare.org/; http://www.pangaea.de).

4 Chronostratigraphy

Ages for most of the cores shown in this paper are derived from the LR04 stack (Lisiecki and Raymo, 2005). The benthic record of IODP Site U1313, the re-occupation of DSDP Site 607, was directly correlated with the stack with most correlation points being isotopic maxima (Voelker et al., 2009). The record of MD01-2446 was correlated

with the Site U1313 curve in the interval where the two overlap and to the LR04 stack for the interval from late MIS 10 to MIS 9. The resulting records are shown in Fig. 2a and their age/depth relations in Fig. 2c.

Establishing the age model for intermediate depth site MD03-2699 was more difficult as the deep water δ^{18}O signal here is modified by the Mediterranean Outflow (MOW) during glacials and glacial inceptions (Voelker et al., 2007). The age model for this core is based on the correlation of its benthic δ^{18}O records to the one of ODP Site 980 (on LR04 time) and two nannofossil events. ODP Site 980 was chosen as reference curve over the LR04 stack as it is from intermediate water depths (Table 1) too. Consequently, water mass signals during times of lower MOW influence at site MD03-2699 were similar at both sites (Fig. 2b). The two nannofossil events (Amore et al., unpubl. data) corroborating the age model are the acme of *Gephyrocapsa caribbeanica* (Flores et al., 2003; Baumann and Freitag, 2004) and the last/highest observed occurrence (LO or HO) of *Pseudoemiliania lacunosa.* The *G. caribbeanica* acme begins in late MIS 14 and therefore helps to constrain the core's basal age. The LO of *P. lacunosa* is placed at the depth of 1895 cm which has an age of 453.6 ka with the current age model, in agreement with (Raffi et al., 2006).

Due to stronger winnowing by the MOW as evidenced by foraminifer sands, sedimentation rates in core MD03-2699 subsided during glacial maxima, especially during MIS 12 (Fig. 2c). Overall, sedimentation rates of core MD03-2699 and IODP Site U1313 are similar, while they are lower in core MD01-2446 (Fig. 2c). Temporal resolution of the planktonic stable isotope records are 100–600 years for IODP Site U1313, 90–1210 years for core MD03-2699 and 280–1820 years for core MD01-2446.

ODP Site 980 records are shown on the LR04 age model of Lisiecki and Raymo (2005) in this paper and the *N. pachyderma* (r) stable isotope records have a temporal resolution of 40 to 3230 years. The age scale of ODP Site 1056 was transferred to LR04 time using the Billups et al. (2004) correlation points between ODP Sites 1056 and 980 (here placed on LR04 time). For ODP Site 1058 we are using the alternative age model of Weirauch et al. (2008) that correlates ODP Site 1058 with ODP

CC BY

Site 677, as this age model results in a better agreement between hydrographic conditions at (I)ODP Sites 1058 and U1313 during MIS 14. Temporal resolution of the *N. dutertrei* stable isotope records varies between 110 to 1830 years for ODP Site 1056 and 40 to 2260 years in ODP Site 1058.

5 Results

5.1 IODP Site U1313

The record of IODP Site U1313 (Fig. 3) spans the interval from 560 to 355 ka fully capturing interglacial MIS 13 and MIS 11 as well as the MIS 14 to 13 deglaciation (Termination VI). MIS 13 and 11 both contain pronounced cooling events that separate intervals of peak warmth (δ^{18}O<1.75‰). *G. inflata* δ^{18}O values show the familiar glacial to interglacial variations with lowest values during the early part of MIS 11 between 417 and 396 ka (MIS 11c). Similarly, MIS 13 contains two warm stages, MIS 13c and 13a, with lowest δ^{18}O values recorded during the early stages. Other than during the distinct cooling events, the range of individual δ^{18}O fluctuations is relatively small in comparison to the pronounced δ^{18}O variability during glacial MIS 12. Termination V is the one of the largest glacial to interglacial transition of the middle Pleistocene while Termination VI is probably one of the smallest (Lisiecki and Raymo, 2005). The *G. inflata* δ^{18}O values of IODP Site U1313 decreased ~1.5‰ and 1‰, respectively. Both events, however, reveal a reversal toward higher δ^{18}O values midway through the transition, similar to the Younger Dryas during the last Termination.

Although MIS 11 may have been the warmest interval of the past 1000 ka, the G. inflata δ^{13}C record contains a maximum in the later stage of MIS 13 (MIS 13a; Fig. 3). High δ^{13}C values are a typical signal for mid-Brunhes planktonic and benthic δ^{13}C records (e.g. Hodell et al., 2003). During MIS 13c and 11c, δ^{13}C values were at a similar level, but on average 0.5‰ lower than during MIS 13a. Terminations VI and V were associated with pronounced δ^{13}C minima.

CC BY

Melting icebergs reached IODP Site U1313, located within the area of high IRD sedimentation during Heinrich events (Hemming, 2004), during all the mid-Brunhes glacials, but IRD deposition was more pronounced and frequent during MIS 12 (Fig. 3). The first IRD event recorded at site U1313 during the transition from MIS 13 to 12 occurred at 490 ka followed by a 23 ka long period with continuous, but not intense IRD sedimentation. After 467 ka, the record reveals four intervals of increased IRD deposition with the last interval exhibiting three short-term maxima. All of the IRD maxima as well as the IRD peak during MIS 10c (isotopic event 10.4) contain dolomite grains (Stein et al., 2009) and are thus interpreted as Heinrich-type ice-rafting events. During MIS 13a IRD deposition ceased for 12 ka (506.4–494.3 ka). During Termination V continuous IRD deposition ended already at 415.9 ka and during MIS 11c melting icebergs did not reach Site U1313 between 410.7 and 399.6 ka (Fig. 6).

5.2 Core MD01-2446

The G. inflata δ^{18}O record of core MD01-2446, the offshore site off Portugal, shows the same features as the Site U1313 record with relative stable conditions during the interglacials and millennial-scale variability during glacial inceptions and glacials (Fig. 4). In contrast to Site U1313 conditions in the thermocline waters were more variable during MIS 13 and cooling during MIS 13b was less. The interval with values <1.75‰ during MIS 11c lasted from 419.4 until 395.6 ka or even 394.3 ka, if one excludes the short excursion down to 1.8‰ at 395.3 ka. During MIS 9e, such light isotope values are observed continuously between 335 and 317 ka. MIS 11c and 9e δ^{18}O values were in the same range and even some values during MIS 13a reached this level (Fig. 4). The MD01-2446 record shows several δ^{18}O oscillations during Terminations VI and IV, while the Termination V sequence looks similar to the Site U1313 record but with less pronounced cooling during the Heinrich-type ice-rafting event.

Also analogous to the Site U1313 record, *G. inflata* δ^{13}C was heaviest during MIS 13a and values during MIS 13c and 11c were in a similar range. In contrast, δ^{13}C values during interglacial MIS 9e were much lower and kept on rising during the

CC BY

interglacial to reach maximum values only during MIS 9d (Fig. 4). δ^{13}C minima during glacials were lower than at Site U1313. In contrast to Site U1313, *G. inflata* recorded a pronounced δ^{13}C minimum between 452 and 443 ka offshore Portugal. During MIS 10, lower δ^{13}C values occurred especially between 351 and 342 ka.

Although Site U1313 received continuous but in comparison to the other glacials small amounts of IRD during MIS 14 (Fig. 3), (coarse) IRD deposition offshore Portugal was nearly negligible and no IRD was deposited during MIS 13 after 523 ka (Fig. 4). During MIS 12, melting icebergs started to reach the Portuguese margin after 472 ka, i.e. significantly later than at IODP Site U1313. The last two IRD peaks in core MD01-2446 during MIS 12 coincided with the last interval of increased IRD deposition at Site U1313 and its Heinrich-type IRD events. At site MD01-2446, however, IRD deposition greatly diminished between the Heinrich-type events. During MIS 10, phases of intensive ice rafting coincided with stadial MIS 10c and with Termination IV. Minor amounts of lithic grains, generally clear quartz grains, were deposited throughout MIS 9e (Fig. 4), especially until 322 ka. However, as the tropical planktonic foraminifera species *G. menardii* is found in the same samples as the quartz grains and mean annual SST further south on the margin exceeded 19°C (Martrat et al., 2007) these grains were more likely deposited by strong westerly winds during the upwelling season than by melting ice. During MIS 11c, coarse lithics were not deposited between 410.8 and 393.6 ka with the exception of one quartz grain found at 404.2 ka that was probably also wind-transported. After 393.6 ka minor amounts of lithics were encountered throughout the glacial inception.

5.3 Core MD03-2699

At nearshore site MD03-2699 the glacial to interglacial pattern that is so clearly evident at the other two sites is more difficult to detect (Fig. 5). While glacial maxima of MIS 12 and 10 are recorded as distinct δ^{18}O maxima and interglacials as distinct minima, glacial inceptions are characterized by relatively large δ^{18}O variability masking a clear

designation into substages. Furthermore, large fluctuations (>0.5‰) in δ^{18}O values are evident during the early stages of MIS 13 (MIS 13c). In fact, Termination VI is entirely masked by high amplitude δ^{18}O variations, and the MIS 13 cool event (isotopic event 13.2) sees a return to glacial-like δ^{18}O values. Warmer thermocline temperatures (δ^{18}O<1.75‰) dominated during interglacial MIS 11c between 417 and 393.6 ka and during MIS 9e from 336.2 to 316.6 ka.

All three glacial inceptions covered by the record reveal millennial-scale oscillations and δ^{18}O values remained relatively low until the subsequent glacial maximum was reached (Fig. 5). Values during the warm phases of these oscillations were in the range of the MIS 13a levels, especially during MIS 12. Also values during interstadial MIS 14b (isotopic event 14.3) reached such levels. During interstadial MIS 9c (311.5–315 ka) thermocline δ^{18}O values (temperatures) were as low (warm) as during MIS 13a or the warm oscillations recorded during MIS 12b and 10b.

Overall, the shape of the δ^{13}C record mimics the pattern described for IODP Site U1313 and site MD01-2446 with heaviest δ^{13}C values recorded during MIS 13 and 11. Contrary to those records heavy δ^{13}C values persisted throughout MIS 12b (Fig. 6). The same is seen during the inception of MIS 10 and in particular during MIS 10c and 10b. Like at site MD01-2446 interglacial MIS 9e is associated with increasing δ^{13}C values that reached higher levels only during MIS 9d and 9c. During MIS 11c the δ^{13}C record shows a stepwise recovery from the minimum during Termination V. The first "plateau" with values generally between 0.75 and 0.9‰ lasted from 416.5 to 401.4 ka, followed by a second maximum with values mainly between 1 and 1.25‰ from 401.1 to 394.4 ka. Also the MIS 13 record of MD03-2699 shows more structure than in the previous records. Although highly variable, early MIS 13c is associated with a maximum in δ^{13}C values, followed by a broad minimum lasting from late MIS 13c to MIS 13b and a subsequent maximum with the highest values (up to 1.47‰) recorded at site MD03-2699 during MIS 13a. The lowest δ^{13}C values of the record were recorded during the colder phases of MIS 14.

Trace amounts of lithics >315 μm were found during MIS 14, early MIS 13c and

CC BY

MIS 13b (Fig. 5). During MIS 12 the first, but minor IRD peak occurred at 470 ka. Continuous IRD deposition started after 442 ka and lasted until 422.8 ka. IRD peaks during this interval coincided with the Heinrich-type events recorded at IODP Site U1313. After this interval with intensive IRD deposition, minor amounts of lithics (mainly quartz grains) were detected until 410 ka. In three levels during MIS 11c (Fig. 6e) 1 or 2 quartz grains were observed, but these grains are most likely wind-transported from the Portuguese coast. A significant IRD peak occurred around 388 ka within MIS 11b (isotopic event 11.24; Figs. 5, 6e). After this first MIS 11 stadial, minor amounts of lithics were deposited on and off throughout MIS 11a (Fig. 6e). As all those periods of lithic grain deposition coincided with the presence of tetra-unsaturated alkenones (Rodrigues et al., 2009), which are linked to fresher surface waters (Bard et al., 2000), the lithics are interpreted as IRD. MIS 10 is associated with another extended period (362.2–333.4 ka) of ice rafting. Maximum IRD concentrations, however, occurred during MIS 10b. A small IRD peak is also associated with stadial MIS 9d.

5.4 Sea surface temperature reconstructions for MIS 10 to 12

Annual mean SST at IODP Site U1313 varied between 7.7 and 20.2°C (Fig. 6b). The coldest SST was recorded during the Heinrich-type ice-rafting events during MIS 12 and 10c (isotopic event 10.4). SST rose quickly after the onset of Termination V increasing by nearly 8.5°C between 427 and 423 ka. During MIS 11c two SST plateaus with values around 18°C are observed with the second plateau, which also experienced minimally warmer SST, coinciding with the interglacial sea level highstand (408–396 ka). During the subsequent glacial inception, the more pronounced cooling occurred during the MIS 11b stadial (isotopic event 11.24; ~390 ka).

At core site MD03-2699 mean annual SST were relatively warm during MIS 12 with 11.7 to 15.8°C (Fig. 6e). SST then dropped to values below 8°C during the Heinrich-type event at the beginning of Termination V. Similar to the *G. inflata* δ^{13}C records the SST data also shows two plateaus for MIS 11c. The first plateau with SST around 17.6°C lasted from 425 to 413.7 ka, followed until 410 ka by an interval with more vari-

CC BY

able SST and some values as low as 16.8°C. The second SST plateau with values exceeding 18°C lasted from 410 to 402.5 ka, but SST dropped permanently below 17.5°C only after 396.6 ka with the transition into stadial MIS 11b. During the glacial inception of MIS 10, the SST record reveals four cold/warm cycles whose amplitude weakened towards MIS 10d (Fig. 6e). MIS 10b was associated with warmer SST that were as warm as the warm oscillations within MIS 11a.

5.5 Comparison to published records

North Atlantic ODP Site 980's $\delta^{18}O$ data was discussed in previous publications (Oppo et al., 1998; McManus et al., 1999) and is shown in Fig. 7. This site's $\delta^{13}C$ record of *N. pachyderma* (r) reveals the lowest $\delta^{13}C$ values during the earliest phase of MIS 12 and during the colder intervals of MIS 10 (Fig. 7). $\delta^{13}C$ levels recorded during interglacials MIS 13a and 11c were similar and about 0.5‰ heavier than those during interglacial MIS 9e. With the onset of the inception of glacial MIS 12 (480 ka), $\delta^{13}C$ values declined continuously towards the MIS 12b minimum (isotopic event 12.2). During the inception of glacial MIS 10, on the other hand, $\delta^{13}C$ values remained relatively high between 390 and 360 ka; levels that frequently exceeded the MIS 9e values. The inception of MIS 10 is nevertheless modified by higher frequency variability.

For western subtropical Atlantic ODP Sites 1056/1058 the *N. dutertrei* stable isotope records are also shown in Fig. 7. *N. dutertrei* records conditions towards the bottom of the seasonal thermocline (Billups et al., 2004) with the highest flux in winter (Deuser and Ross, 1989). Thus its living conditions are comparable to those of *G. inflata* (Fairbanks et al., 1980; Deuser and Ross, 1989; Cléroux et al., 2007). Contrary to the other sites in this study, heaviest $\delta^{13}C$ values were not concurrent with the sea level highstands of MIS 13a and 11c, both of which exhibit relatively low values (Fig. 7). Times with highest $\delta^{13}C$ values coincided with late MIS 14 to 13c and with stadial MIS 11b. For most of the record covered by Site 1056 (MIS 12–10; darker green line in Fig. 7), $\delta^{13}C$ values varied between 0.75 and 1.5‰ and dropped to a longer lasting minimum only during the glacial maximum of MIS 10 (isotopic event 10.2). Thus there was no

CPD
5, 1553–1607, 2009

major difference between glacial MIS 12 and warm MIS 11. A similar pattern is seen at ODP Site 1058 where interglacial MIS 13a and higher values during glacial MIS 12 reached comparable levels (lighter green line in Fig. 7). However, δ^{13}C values declined from MIS 13a to the MIS 12 glacial maximum (isotopic event 12.2), despite of millennial-scale variability overprinting the record.

6 Discussion

6.1 Hydrographic conditions off Portugal

Although core sites MD03-2699 and MD01-2446 are located only about 170 km apart, their *G. inflata* δ^{18}O records are very different in that the nearshore site displays large and rapid fluctuations suggesting very different hydrographic conditions, especially during the glacial inceptions and glacials. The two sites are more similar during interglacial MIS 9e, 11c and 13a, but with core MD03-2699 revealing slightly lower values, thus indicating warmer waters (Figs. 7, 8). We suggest that the higher variability in the δ^{18}O record of core MD03-2699 reflects variations in upwelling of deeper waters into the thermocline.

Regarding the single or double point δ^{18}O maxima recorded during the peak warmth of MIS 11 in core MD03-2699, duplicate analyses confirmed the heavier δ^{18}O values and the accompanying δ^{13}C values are not analytical outliers. Furthermore, parallel measurements in *Orbulina universa* (Voelker et al., unpubl.data) as well as any of the other proxy records (e.g. XRF data, carbonate; Voelker et al., unpubl.data) existing for this core do not contain any sign of reworking or core disturbances at or around those levels. Thus the *G. inflata* values are seen as to be correct and appear to reflect the presence of very cold wintertime thermocline waters. Since the cold spell at 412.65 ka is associated with seven coarse lithic (IRD) grains (Fig. 6e) the source for the cooling seems to be advection of ice-transporting subpolar waters. At the beginning of the younger cooling event that lasted from 401.7 to 401.4 ka, one quartz grain was found.

CC BY

As this cooling of about 4°C occurred during the MIS 11c sea-level highstand, upwelling of the deeper subpolar ENACW induced by strong winds – thus making the lithic grain a dust grain – is more likely the cause for the cooling. The short cooling at 326.3 ka during MIS 9e and the high variability in both δ^{18}O and δ^{13}C during MIS 13c and b are probably also related to the influence of upwelled waters. Increased productivity during MIS 13c, most probably related to upwelling, is indicated by higher organic carbon concentrations (Voelker et al., unpubl. data). While the interglacial δ^{18}O levels are similar at the two sites and for MIS 11c also in agreement with those recorded for core MD01-2443 (Fig. 6f; de Abreu et al., 2005), *G. inflata* δ^{13}C values at site MD01-2446 are generally higher than at site MD03-2699 indicating that more nutrients were available in the offshore waters either because of lower nutrient consumption (open ocean vs. upwelling regime) or because the waters offshore had already higher preformed nutrient concentrations.

The alkenone-derived SST (Fig. 6e) indicates extremely stable mean annual surface water temperatures during MIS 11c in the nearshore waters off Portugal. The new record from core MD03-2699 agrees well with the one of core MD01-2443 (Fig. 6g; Martrat et al., 2007). Both records show two plateaus within MIS 11c and a short minimum prior to the second, warmer plateau coinciding with the MIS 11c sea-level highstand (note that the minimum in MD01-2443 is shifted towards older ages with the Tzedakis et al. (2009) age model (Fig. 6g), while with the de Abreu et al. (2005) age model (not shown) the minima are aligned). Such a strong SST stability over thousands of years is not seen in the NAC waters at IODP Site U1313 (Fig. 6b) where temperatures, however, reached values similar to those off Portugal. While not as clearly marked as at the Portuguese sites, Site U1313 also recorded two intervals with warmer SST during MIS 11c separated by a minimum, which at 41° N was more pronounced. More variable conditions in the NAC waters are probably linked to admixing of subpolar surface waters, especially during the first MIS11c temperature plateau when hydrographic conditions in the Nordic Seas (Helmke and Bauch, 2003) and the Arctic Ocean (Knies et al., 2007), thus in the subpolar and polar regions, were still unstable

CPD
5, 1553–1607, 2009

due to freshwater release. The stability in annual mean temperatures off Portugal, on the other hand, must be related to a dominant influence of the subtropical AzC and IPC waters and thus confirm that the hydrographic (winter-time) situation off Portugal during MIS 11c was similar to the Present (Fig. 1b). Since the temperature trends were similar along the different North Atlantic surface currents it appears that the signal originated in the tropical/subtropical regions of the Atlantic Ocean and was advected northwards. This agrees with the observation of Kandiano and Bauch (2007) that northward advection of subtropical waters is causing the SST optimum at Rockall Plateau site M23414. Tropical planktonic foraminiferal species also contributed significantly to the MIS 11c fauna of core MD01-2443 (de Abreu et al., 2005). In cores MD03-2699 and MD01-2446, the deeper dwelling tropical species *Globorotalia menardii* and *Sphaeroidinella dehiscens*, both of which do not occur in the modern fauna off western Iberia (Salgueiro et al., 2008), were found in MIS 11c (Fig. 6d) and 9e samples. Thus it appears that within the North Atlantic's eastern boundary system heat was transported northward not only by the IPC, but also at subsurface level through an enhanced contribution of the eastern boundary undercurrent to the IPC's subsurface component. This enhanced flux of tropical subsurface waters, which are nutrient poor, could also contribute to the lower *G. inflata* δ^{13}C values at site MD03-2699. It, furthermore, confirms that heat flux into the North Atlantic was at its maximum during the mid-Brunhes (Berger and Wefer, 2003).

MIS 11c interglacial conditions off Portugal ended around 395 ka with the onset of the 11b stadial (isotopic event 11.24). Cooling during this stadial was gradual and coldest conditions were reached only towards the end of the stadial coincident with IRD maxima around 388 ka (Figs. 4, 6). Even though site MD03-2699 received more IRD, δ^{18}O-inferrred surface water-cooling seems to have been similar between the two sites (Fig. 8d). Since SST at MD01-2443, located just about 1 degree further south than MD03-2699, reveal less cold temperatures, subtropical IPC waters probably still influenced the southern margin and their presence might have enhanced iceberg melting near site MD03-2699. The pollen record of core MD01-2447 at 42° N (Desprat et

CC BY

al., 2005) confirms maximum cooling towards the end of the stadial also for northern Iberia, but more importantly it shows that cooling along with the IRD peaks recorded at site MD03-2699 and MD01-2446 was restricted to the winters. Since melting icebergs and colder surface waters reached the western Iberian margin much later than IODP Site U1313 (Figs. 3, 6a, b) or ODP Site 980 (Fig. 6c), where IRD deposition peaked 1000 years prior but persisted until the end of the stadial (Oppo et al., 1998), a latitudinal front must have existed north of the Iberian Peninsula. In addition, it appears that it took ≥1000 years of meltwater flux into the subpolar and northern transitional regions to weaken AMOC enough to push this front as far south as 39° N.

MIS 11a and thus the glacial inception of MIS 10 is marked by four stadial/interstadial cycles, the first interstadial of which is associated with isotopic event 11.23 (Figs. 3–6). The cycles are best depicted in the alkenone SST records (Fig. 6b, e). Cooling during the second stadial is much stronger on the northern (Desprat et al., 2005) and middle Iberian margin (MD03-2699) than in the NAC waters (IODP Site U1313). Therefore a European or Scandinavian source for the cooling is more likely than advection with the NAC from the western subpolar gyre, the typical source region for ice-rafting events during MIS 3. Such an eastern source region is supported by the stronger IRD signal at ODP Site 980 (Fig. 6c; Oppo et al., 1998) than at IODP Site U1313, even given the differences in the IRD size fraction. The subsequent stadials had only small impacts on the SST at site MD03-2699, but were associated with short, but strong coolings in the *G. inflata* δ^{18}O record indicating the presence of colder surface waters during some of the winters (a more detailed discussion of the δ^{18}O data follows below). The cold temperatures recorded by *G. inflata* might be linked to the ones recorded in the MD01-2443 alkenone record (Fig. 6g; assuming an offset due to age models for stadial III). However, since alkenones represent annual mean temperatures and thus smooth a more seasonal signal like the *G. inflata* δ^{18}O data and since MD01-2443's cold alkenone SST are not reflected in the faunal based SST (de Abreu et al., 2005), these for this latitude unusually cold SST outside of a Heinrich event or glacial maximum need to be confirmed by other records from the northern Iberian margin or the Bay of Bis-

CPD
5, 1553–1607, 2009

caye, i.e. regions closer to potential sources for such cold waters. Such confirmation is especially important because stadials II and III did not coincide with Heinrich-type events (Hodell et al., 2008; Stein et al., 2009) and such strong coolings are (so far) not detected in other records either along the NAC path – IODP Site U1313 (Fig. 6a, b) and core M23414 (Kandiano and Bauch, 2003) – or more locally in the planktonic δ^{18}O records of cores MD01-2446 (Fig. 4) and MD01-2447 (Desprat et al., 2005). In addition, at ODP Site 980 ice-rafting and cooling as indicated by the presence of *N. pachyderma* (s) was much lower during stadial III than stadial II (Fig. 6c). The pollen based terrestrial temperature records for core MD01-2447 also reveal only minor cooling during the younger stadials (Desprat et al., 2005), conform with the MD03-2699 SST record. Thus for the moment the SSTs recorded in core MD03-2699 appear to be more realistic for the western Iberian margin during MIS 11a than the MD01-2443 signal.

With the onset of MIS 11a the *G. inflata* δ^{18}O and δ^{13}C records of core MD03-2699 start to diverge from the offshore signal at site MD01-2446 (Fig. 8d). For most of the glacial inception, δ^{18}O values in core MD03-2699 stayed low, while values in core MD01-2446 increased as is to be expected with gradual cooling and increasing ice volume. The difference between these two relative closely located core sites can only be caused by a strong hydrographic front. Because *G. inflata* is reflecting winter mixed-layer conditions this front must have been the northward trending subtropical front, in a manner similar to the present when the front allows warmer subtropical water to flow across the location of core MD03-2699 (Fig. 1b). The strong IPC influence on the southwestern margin is confirmed by the *G. inflata* δ^{18}O values and warm SST of core MD01-2443 (Fig. 6f, g; de Abreu et al., 2005), which, with the exception of the unusually high values between 375 and 381 ka, have levels similar to those of core MD03-2699. The signal at offshore site MD01-2446, on the other hand, agrees well with the NAC record of IODP Site U1313 (Fig. 8c) and therefore in the PC's source waters. The northward extending subtropical front and thus the dominant IPC influence on nearshore waters off Portugal persisted into the glacial. Only during those

CC BY

times when *G. inflata* δ^{18}O values in core MD03-2699 became temporarily higher and reached MD01-2446 levels (Fig. 8d), like during stadials II and III, did the front not exist and colder waters also penetrated into the nearshore regions. During early MIS 10 the subsurface component of the IPC was strengthened again with deep dwelling tropical foraminifer species (Fig. 6d) being advected to the mid-latitude nearshore Portuguese margin. The increased (temporary) subsurface northward heat flux could explain why mean annual SST and the winter mixed layer at site MD03-2699 were hardly impacted by the Heinrich-type event during stadial MIS 10c (isotopic event 10.4), even though melting icebergs reached this site (Figs. 5, 6e). Since the signals for warmer surface to subsurface waters and IRD deposition occur in the same levels, seasonality at site MD03-2699 must have been very high during MIS 10.

The pattern with a strong subtropical front separating sites MD03-2699 and MD01-2446 and with subtropical IPC waters dominating the nearshore waters of the Portuguese margin is not only seen for the glacial inception of MIS 10, but also during MIS 12 and with lesser intensity during MIS 14b (isotopic event 14.3) and the glacial inception starting with stadial MIS 9d (Fig. 8d). Therefore the presence of a northward extending subtropical front off Portugal is a typical feature for the glacial inceptions and glacials of the mid-Brunhes period. For the transition from MIS 13a to 12a four short-term colder episodes are detected in the *G. inflata* δ^{18}O record of core MD03-2699. Values during those times did not, however, reach the colder MD01-2446 levels (Fig. 8d), except for the short IRD event at 470 ka (Fig. 5) that like stadial MIS 11b also had more likely an eastern source because a pronounced IRD peak is recorded at site M23414 (Kandiano and Bauch, 2003) and ODP Site 980 (Oppo et al., 1998) but not at IODP Site U1313 (Fig. 3). Overall, wintertime hydrographic conditions in the nearshore waters off Portugal appear to have been warmer and more stable during MIS 12 than during the subsequent glacial inception. Such temperature "stability" points to a strong influence of the subtropical Azores Current in this region and is conform to evidence from the western Mediterranean Sea. There planktonic δ^{18}O records of ODP Sites 976, 977 and 975 (Pierre et al., 1999; von Grafenstein et al., 1999) reveal

CPD
5, 1553–1607, 2009

significantly warmer surface waters during glacial MIS 12 and 14 than during MIS 10. Some of the waters advected polewards with the IPC might actually be responsible for the continuously warm SST at ODP Site 980 during the early MIS 12 (McManus et al., 1999), a signal quite different from the NAC and PC records of IODP Site U1313 and core MD01-2446 that depict several smaller scale warm/cold oscillations throughout MIS 12b (Figs. 3, 4).

During late MIS 12, minimum alkenone SST of core MD03-2699 are similar to minimum temperatures recorded during early MIS 10 (Fig. 6e). SST in nearshore waters off Portugal, however, rose continuously towards the deglaciation. During the MIS 12 glacial maximum at 430 ka a SST gradient of $\geq$6°C existed between IODP Site U1313 and MD03-2699 (Fig. 6b and e, respectively) indicating that a front – either just the subtropical front off Portugal or even the polar front – separated the surface waters in this mid-latitudinal band. The trend of rising SST off Portugal was abruptly interrupted by the significant cooling associated with the Heinrich-type ice-rafting event around 427 ka at the onset of the deglaciation (Hodell et al., 2008; Stein et al., 2009). Without this event, SST off Portugal would probably have increased gradually towards MIS 11. This Heinrich-type event had a major impact on the hydrography in the North Atlantic, even leaving a fresher water signal in the *G. inflata* records of core MD01-2446 (low δ^{18}O values contemporary with light δ^{13}C values; Fig. 4), and led to a temporary AMOC shut down (Voelker et al., 2009), just like its younger counterparts. A Heinrich-type event is also associated with Termination IV as evident by core MD01-2446's records (Fig. 5), where the presence of melting icebergs led to strong oscillations in the planktonic δ^{18}O values.

6.2 Basinwide surface water circulation and linkages to thermocline water sources

Both the PC and the IPC also have a subsurface component of subpolar or subtropical waters, respectively, whose properties contribute to those in the deep winter mixed layer in which deeper dwelling foraminifer like *G. inflata* calcify their tests. By tapping

CC BY

into subsurface waters deep winter mixing replenishes the nutrients available in the upper water column. Since δ^{13}C values measured in planktonic foraminifer tests are related to nutrient concentrations (Broecker and Peng, 1982; Ortiz et al., 1996) we are using them to trace the subsurface/mode waters in the North Atlantic. Such an approach is facilitated by the fact that the subpolar mode water is formed during winter along the NAC branches around the Rockall Plateau (Brambilla and Talley, 2008) and thus in close vicinity to ODP Site 980. Because the mode water is directly advected southward with the Portugal current the transport way is relatively short minimizing the time during which the δ^{13}C signal could be modified. Furthermore, the selected planktonic foraminifer species represent conditions in winter and thus prior to the spring blooms and upwelling season during which the δ^{13}C would be altered due to nutrient consumption. The comparison between sites focuses on trends and not on absolute values because the δ^{13}C values of the different species were not corrected to dissolved inorganic carbon (DIC) levels (except for the ODP Site 980 *N. pachyderma* (r) values in Fig. 8a and b where the correction was added to minimize the plot's δ^{13}C range). Thus only the δ^{13}C values of the *G. inflata* based records of IODP Site U1313, MD01-2446 and MD03-2699 are directly comparable.

In the direct comparison it becomes clear that the offshore core MD01-2446 is very similar to North Atlantic IODP Site U1313 (Figs. 7, 8c) indicating that for most of the studied interval hydrographic conditions, i.e. temperature and salinity properties, were not much different in the NAC and the PC. For most of the time the *G. inflata* δ^{13}C values at both sites were comparable and generally heavier than at site MD03-2699. However, there were also intervals when the two open ocean records diverged. One such example is the interstadial associated with isotopic event 11.23 when warm conditions in the NAC at IODP Site U1313 lasted longer than in the PC record of core MD01-2446 that is more comparable with the NAC record at ODP Site 980 (Figs. 7, 8a–c). Thus it might be that the NAC's main flow path was shifted more southward than its current position (Fig. 1) and that the NAC waters reaching the Rockall Plateau and feeding the PC were already modified by entrainment of subpolar waters. A strong

CC BY

linkage in water mass conditions between the Rockall Plateau NAC branch and the PC is confirmed by the δ^{13}C records (Figs. 7, 8b). This relationship is especially evident during MIS 12 when the MD01-2446 δ^{13}C data follows the ODP Site 980 record, especially the pronounced δ^{13}C minimum during early MIS 12 that is only recorded at these two sites (Fig. 7). Thus it appear that the poorly ventilated surface to subsurface waters advected southward with the PC during MIS 12 were formed near or above the Rockall Plateau, probably in regions similar to those of modern subpolar mode water formation (Brambilla and Talley, 2008). Enhanced influence of eastern basin waters is also consistent with a stronger imprint of the 470 ka IRD event in these records. MIS 12 δ^{13}C values at IODP Site U1313, on the other hand, stayed fairly constant despite the strong temperature and salinity oscillations indicated by the δ^{18}O data and the presence of melting icebergs (Fig. 3). Thermocline waters in this region were better ventilated than in the eastern basin indicating that Gulf Stream waters (ODP Site 1056 and 1058; Fig. 7) still reached this latitude, in agreement with the relative warm SST during most of MIS 12 (Stein et al., 2009) that also imply northward heat advection. The persistent nutrient supply by the thermocline waters supported increased phytoplankton production near Site U1313 (Stein et al., 2009). Even though supported only by isotope data for early MIS 10, the same pattern with well ventilated thermocline waters supporting high productivity (Stein et al., 2009) is also seen then, while the MD01-2446 and ODP Site 980 records indicate that the Rockall Plateau was – similar to MIS 12 – the source region for the PC waters (Fig. 8b). Thus while during mid-Brunhes glacial intervals Gulf Stream derived NAC waters penetrated at least until 41° N in the western basin, their influence was diminished in the eastern basin. Especially during early MIS 12, the position of the polar front appears to have been tilted in the North Atlantic reaching further to the south in the eastern than western basin. The glacial differences are also well seen in the scatter plots (Fig. 9a) with divergences towards higher/lower δ^{13}C values in IODP Site U1313 and core MD01-2446, respectively. However, these plots also reveal that during most of the time, in particular during the interglacial intervals (lower δ^{18}O values), conditions at the three sites influenced by the NAC and PC were not much

different (Fig. 9b); thus making the NAC like today the dominant hydrographic feature in the mid-latitude North Atlantic.

Although the NAC and PC records at IODP Site U1313, ODP Site 980 and site MD01-2446 agree well, there is one interval when the MD01-2446 record diverges from the others and this is the δ^{13}C minimum associated with Termination V (Fig. 8a–c). During the onset of the deglaciation δ^{13}C levels are similar at the three sites. However, while the δ^{13}C minimum at Site U1313 lasted for 10 ka, which is similar to ODP Site 980 (Fig. 8a), at site MD01-2446 it ended after only 5 ka, which is also sooner than at site MD03-2699 (Fig. 8d). The late glacial and deglacial δ^{13}C minima are generally linked to poorly ventilated and thus nutrient-rich water masses such as Subarctic Intermediate Water (Venz et al., 1999) or Antarctic Intermediate Water, the later of which penetrated as far north as 61.5° N during the last deglaciation (Rickaby and Elderfield, 2005). The presence of better ventilated waters at site MD01-2446 therefore implies the formation of well ventilated mode water, may be similar to the formation of subtropical NACW along the Azores front during modern winters, somewhere south of 41° N and offshore of western Iberia. A different length of the deglacial δ^{13}C minimum is not seen for Termination VI, when it lasted about 8 ka at both IODP Site U1313 and site MD01-2446, or for Termination IV, when lesser ventilated surface to subsurface waters were present in the eastern North Atlantic basin (ODP Site 980, MD01-2446, MD03-2699; Fig. 8b, d) also throughout the subsequent interglacial and thus for almost 20 ka. Hydrographic conditions during MIS 9e were different than during the other interglacial intervals. This is not only evidenced by the prolonged δ^{13}C minimum but also by the persistent, if low presence of the polar species *N. pachyderma* (s) in the planktonic foraminifer fauna off Iberia during the first half of the interglacial (de Abreu et al., 2005; Desprat et al., 2009). Based on the deciduous quercus pollen record of core MD03-2697 at 42° N (Desprat et al., 2009) the climatic optimum occurred during the second half of the interglacial – comparable, but not equal to the 2nd warmer phase of MIS 11c. Warmer surface waters in the PC and NAC during the 2nd half of the interglacial are supported by the δ^{18}O record of core MD01-2446 and the alkenone SST

CC BY

record of IODP Site U1313 (Stein et al., 2009). The prolonged δ^{13}C minimum implies advection of poorly ventilated waters into the mid-latitude North Atlantic. These waters were most likely Subarctic Intermediate Water since the records of ODP Site 982 on the northern Reykjanes ridge (57.5° N) reveal the same δ^{13}C minimum accompanied by persistent, but low input of IRD (Venz et al., 1999). Thus ice-bearing arctic waters must have penetrated from the Nordic Seas southward across the Iceland-Faeroe ridge into the subpolar gyre where they mixed with the NAC waters since this is one of the region were subpolar mode water is formed at Present (Brambilla and Talley, 2008). Besides the poor ventilation the advection of subpolar waters to the Iberian margin had no impact because mean annual and summer SST in the nearshore band stretching from site MD01-2443 (Martrat et al., 2007) over MD03-2699 (Rodrigues et al., 2009) to MD03-2697 (Desprat et al., 2009) exceeded 18°C. Thus the contributions of *N. pachyderma* (s) to the planktonic foraminifer fauna are more likely an indicator for increased upwelling of the colder subpolar ENACW off Iberia and thus stronger winds because only those would cause subpolar ENACW to be upwelled south of 40° N. With windier conditions during early MIS 9e, the lithic grains found at site MD01-2446 (Fig. 4) could be wind transported.

As already mentioned above the δ^{13}C values in records for NAC and PC waters were mostly heavier than at site MD03-2699 in agreement with subpolar source waters being better ventilated than subtropical ones. Given that the δ^{18}O and SST data implies a strong IPC influence on the latter record, the δ^{13}C values of core MD03-2699 should show some resemblance to those values recorded in the subtropical Gulf Stream waters at ODP Sites 1056 and 1058 (Figs. 7, 8e). Based on the scatter plots (Fig. 9c, d) there is only minor overlap between the records from the western and eastern side of the North Atlantic basin and that seems mainly to be restricted to MIS 11 as implied by the MD01-2443 data (Fig. 9d). The *N. dutertrei* δ^{13}C record of ODP Site 1056 shows a similar pattern to core MD03-2699 during MIS 11c with lighter values indicating relatively more nutrients during the early phase and heavier values during the later phase of the interglacial (Fig. 8e). Consequently, this two-step feature in nutri-

CC BY

ent concentrations is a subtropical gyre signal. Trends and even absolute $\delta^{13}C$ values were also similar at ODP Sites 1056 and 1058 and site MD03-2699 between 495 and 440 ka and after 350 ka (Fig. 8e); thus during those glacial times, when SSTs and $\delta^{18}O$ data of core MD03-2699 indicate a strong subtropical water influence. The good correspondence during MIS 12 might indicate that cross-Atlantic transport with the AzC was strong with little admixing of transitional waters. This enhanced AzC (heat) flux towards the southern Iberian margin would also explain why MIS 12 is much warmer in western Mediterranean Sea records than MIS 10 (Pierre et al., 1999; von Grafenstein et al., 1999). During the inception of MIS 10, nutrient concentrations at site MD03-2699 were higher than at ODP Site 1056 indicating that the Gulf Stream waters were greatly modified before reaching the western Iberian margin, if they contributed to the subsurface waters there at all. The $\delta^{13}C$ records between the two sites also diverged during MIS 13c and b, when upwelling from either subtropical or subpolar ENACW influenced site MD03-2699. The records were also decoupled during the glacial maximum of MIS 12, when the subtropical front did not separate waters at site MD03-2699 from those recorded in core MD01-2446 and subpolar waters influenced the western Iberian margin.

6.3 Comparison of the interglacials

The new records from the mid-latitude North Atlantic confirm MIS 11c to be a long and relative stable interglacial in comparison to either MIS 13 or MIS 9. Especially the NAC and PC waters experienced only minor changes in the hydrographic conditions and nutrient levels. Thus conditions in the mid-latitude North Atlantic were comparable to those of ODP Site 980 (Oppo et al., 1998; McManus et al., 2003). Based on the $\delta^{18}O$ records hydrographic conditions in those waters were also stable during MIS 9e, while MIS 13c and 13a experienced some small-scale oscillations and consequently less stable conditions (Fig. 7). MIS 13c and 13a are also confirmed to have been colder in than the subsequent interglacials with only short intervals during MIS 13a

CC BY

reaching δ^{18}O values comparable to MIS 11c or 9e levels (Figs. 4–6). In the sites affected by subtropical waters (ODP Sites 1056 and 1058; MD03-2699) variability in the surface water properties was slightly higher during MIS 11c and 9e than in the NAC and PC records, while MIS 13 appears more stable in the Gulf Stream waters (Figs. 7, 8e). At site MD03-2699, on the other hand, MIS 13c and 13a were quite different. Hydrographic conditions during MIS 13c were highly variable due to intense upwelling (see Sect. 6.1), but were more stable and comparable to ODP Site 1058 during MIS 13a (Fig. 8e).

Overall, MIS 11c and 9e appear to have experienced comparable temperature and salinity conditions in the mid-latitude North Atlantic. However, there is one major difference and that is the ventilation of the surface to subsurface waters and their impact on the AMOC. While no impact of the poorly ventilated and potentially fresher waters during MIS 9e is seen in the planktonic δ^{18}O records presented here, they affected the ventilation of the deeper North Atlantic Deep Water (NADW) as evidenced by the benthic isotope record of IODP Site U1308 (Hodell et al., 2008), where well ventilated NADW at 3870 m water depth was only recorded after 323.5 ka, and of core MD01-2446 (Voelker, unpublished data), where until 325 ka NADW ventilation was highly variable. Because the upper NADW as recorded at ODP Site 980 (McManus et al., 1999) was well ventilated, only the deeper branch was affected – either because the Iceland-Scotland Overflow Waters (ISOW) exiting from the Nordic Seas were poorly ventilated or AMOC was shallower during early MIS 9e. Anyhow, a shallower AMOC or poorly ventilated ISOW sets MIS 9e apart from MIS 11c, when AMOC was so strong already early within the deglaciation that after 426 ka well ventilated NADW penetrated as deep as 3870 m (Hodell et al., 2008; Voelker et al., 2009).

The new records extend the region with stable temperature conditions during MIS 11c down to 39° N and confirm that overall hydrographic conditions in the North Atlantic basin were similar to today. Some new insights into hydrographic conditions in the subtropical gyre could be gained from the records of core MD03-2699. They are:

CC BY

1. the existence of two SST plateaus with the second period experiencing slightly warmer temperatures and coinciding with the sea level highstand

2. within the respective plateaus very stable SST in the nearshore waters off Portugal lasting several thousands of years

3. increased northward heat flux of subsurface tropical waters with the eastern boundary undercurrent, especially during the early phase of the interglacial

4. a two step evolution in planktonic $\delta^{13}C$ indicating poorer ventilated subtropical waters during the early phase and better ventilated ones during the second phase; the transition in $\delta^{13}C$ occurred during the sea level highstand and thus later than the transition to warmer SST

5. the formation of well ventilated mode waters in the vicinity of core MD01-2446 during transition from glacial MIS 12 to interglacial MIS 11c.

7 Conclusions

By combining the records of six core sites spanning the latitudes from 32 to 55.5° N and the major surface water currents linked to the subtropical and transitional waters in the North Atlantic Ocean we are able to trace hydrographic conditions from MIS 9 to 14. Overall, planktic foraminiferal $\delta^{18}O$ values and alkenone derived SSTs indicate that surface water temperature and salinity conditions during the interglacials MIS 11c and MIS 9e were not much different and very stable along the NAC and PC. Surface water ventilation, on the other hand, differed with MIS 9e being associated with poorly ventilated surface waters that impacted the deeper branch of the AMOC. In the eastern boundary system off Portugal northward heat flux of tropical waters with the subsurface undercurrent is observed during MIS 11c and MIS 10 as indicated by the presence of tropical species. During early MIS 11c these northward advected (sub)tropical waters even reached the Rockall Plateau (Kandiano and Bauch, 2007). Along with

CC BY

the enhanced northward heat flux hydrographic conditions in the offshore waters off Portugal were such that well ventilated mode waters were formed during the glacial to interglacial transition. So far these mode waters have only been recorded at site MD01-2446 and it remains to be seen in the future if their impact was locally restricted. MIS 13 is confirmed as colder than the subsequent interglacials and except for site MD03-2699 conditions during MIS 13c and 13a were not much different along the major currents. Due to apparently strong upwelling during MIS 13c the planktonic isotope records of core MD03-2699 experienced pronounced variability, while conditions during MIS 13a were relative stable and comparable to those in the Gulf Stream. Overall, it appears that conditions in the mid-latitude North Atlantic were not much different during MIS 11c than during MIS 9e and, if one neglects the generally lower temperatures, also during MIS 13a. Current pathways and associated fronts were similar to today during all the interglacials. The difference between the interglacials lies in the ventilation of the subsurface waters. Here MIS 9e stands apart because the continuous admixing of arctic waters into the transitional waters of the mid-latitude North Atlantic.

Based on the closely spaced core sites MD03-2699 and MD01-2446 it is evident that a strong hydrographic front existed off Portugal, especially during the glacial inceptions and glacials. This front appears to have been equal to the northward extending subtropical front that exists during modern winters (Fig. 1b). East of the front, i.e. in the nearshore waters off Portugal, a strong influence of subtropical waters is recorded at sites MD03-2699 and MD01-2443. Given this overprint of subtropical waters caution should be taken to interpret surface water records from nearshore sites off Portugal as basin-wide signals, at least for the mid-Brunhes interval studied here. Accordingly, the pronounced SST stability recorded in these waters during MIS 11c might be more typical for the subtropical gyre than a Gulf Stream/NAC signal (Fig. 6). Future records off NW Iberia and off NW Africa, i.e. up- and downstream, might help to shed some light onto this question. The hydrographic front disappeared sporadically during stadials of the glacial inception of MIS 10, but cooling episodes in the nearshore waters were much shorter than those recorded offshore (Figs. 7, 8d).

CPD
5, 1553–1607, 2009

Increased heat transport with the AzC across the Atlantic is also seen during MIS 12 when $\delta^{13}C$ records of ODP Sites 1056 and 1058, representing Gulf Stream waters, and of core MD03-2699 were most similar (Fig. 8e). The alkenone SST record of core MD03-2699 confirms relative warm waters at this site and warming from the glacial maximum to the interglacial would probably have been continuously if it had not been interrupted by a Heinrich-type ice-rafting event at the onset of the deglaciation that left a freshwater signal in the offshore waters at site MD01-2446. Cooling during this event is comparable to the cooling observed during younger Heinrich events (e.g. de Abreu et al., 2003). While the nearshore waters off Portugal had a subtropical source during MIS 12, the offshore waters were derived from the Rockall Plateau region as the close correspondence between the records of ODP Site 980 and core MD01-2446 reveal (Fig. 8b). The surface waters in the eastern basin were poorer ventilated than those in the western basin (IODP Site U1313), even though the western basin experienced stronger salinity oscillations linked to more frequent ice-rafting events. Thus during most of MIS 12 NAC waters still reached IODP Site U1313, confirmed by the SST record (Stein et al., 2009), but did not enter into the eastern basin. Consequently, during MIS 12 the position of the polar front was tilted reaching further south in the eastern basin and coming in close contact with the subtropical front off Portugal.

Acknowledgements. This study used samples provided by the Integrated Ocean Drilling Program (IODP) and by the British Ocean Sediment Core Research Facility (BOSCOR). The Fundação para a Ciência e a Tecnologia (FCT) through the PORTO (PDCT/MAR/58282/2004) and SEDPORT projects (PDCTM/40017/2003), and postdoctoral (SFRH/BPD/21691/2005) and PhD (SFRH/BP/13749/2003) fellowships funded A. V. and T. R. Coring of MD03-2699 was made possible through a European Access to Research Infrastructure grant. We thank IPEV, Yvon Balut and the captain and crews of R/V Marion Dufresne for their support in retrieving the two Calypso cores. Special thanks go to Monika Segl (Marum, University Bremen) for the measuring of the isotope samples, to Lucia de Abreu for sampling core MD01-2446, and to Miguel Reis of the ITN in Lisbon for access to the freeze dryer in his lab. The staff of the DGM lab and J. P. Ferreira and B. Montanari are greatly appreciated for their support in sampling and sample preparation. U. Paczek, M. Ferreira, B. Montanari and C. Trindade helped with the

picking of some of the stable isotope samples.

References

Alvarez-Salgado, X. A., Figueiras, F. G., Perez, F. F., Groom, S., Nogueira, E., Borges, A. V., Chou, L., Castro, C. G., Moncoiffe, G., and Rios, A. F.: The Portugal coastal counter current off NW Spain: new insights on its biogeochemical variability, Prog. Oceanogr., 56, 281–321, 2003.

Amore, F. O., Flores, J. A., Filippelli, G. M., Sierro, F. J., Voelker, A. H. L., and Rodrigues, T.: Coccolithophore record during the Middle Pleistocene in the North and South Atlantic: Productivity and Dissolution patterns, Mar. Micropalentology, in preperation.

Bard, E., Rostek, F., Turon, J. L., and Gendreau, S.: Hydrological Impact of Heinrich Events in the Subtropical Northeast Atlantic, Science, 289, 1321–1324, 2000.

Bassinot, F. C., Labeyrie, L. D., Vincent, E., Quidelleur, X., Shackleton, N. J., and Lancelot, Y.: The astronomical theory of climate and the age of the Brunhes-Matuyama magnetic reversal, Earth Planet. Sc. Lett., 126, 91–108, 1994.

Bauch, H. A., Erlenkeuser, H., Helmke, J. P., and Struck, U.: A paleoclimatic evaluation of marine oxygen isotope stage 11 in the high-northern Atlantic (Nordic seas), Global Planet. Change, 24, 27–39, doi:10.1016/S0921-8181(99)00067-3, 2000.

Baumann, K. H. and Freitag, T.: Pleistocene fluctuations in the northern Benguela Current system as revealed by coccolith assemblages, Mar. Micropaleontol., 52, 195–215, doi:10.1016/j.marmicro.2004.04.011, 2004.

Berger, W. H. and Wefer, G.: On the Dynamics of the Ice Ages: Stage-11 Paradox, Mid-Brunhes Climate Shift, and 100-ky Cycle, in: Earth's Climate and Orbital Eccentricity: the Marine Isotope Stage 11 Question, edited by: Droxler, A. W., Poore, R. Z., and Burckle, L. H., Geophysical Monograph, American Geophysical Union, Washington, D.C., 41–59, 2003.

Billups, K., Chaisson, W., Worsnopp, M., and Thunell, R.: Millennial-scale fluctuations in subtropical northwestern Atlantic surface ocean hydrography during the mid-Pleistocene, Paleoceanography, 19, no.2, PA2017, doi:10.1029/2003PA000990, 2004.

Billups, K., Lindley, C., Fisler, J., and Martin, P.: Mid Pleistocene climate instability in the subtropical northwestern Atlantic, Global Planet. Change, 54, 251–262, 2006.

Brambilla, E. and Talley, L. D.: Subpolar Mode Water in the northeastern Atlantic: 1. Averaged

properties and mean circulation, J. Geophys. Res., 113, C0425, doi:10.1029/2006JC004062, 2008.
Broecker, W. S. and Peng, T.-H.: Tracers in the Sea, Tracers in the Sea, ELDIGIO Press, Lamont-Doherty Geological Observatory, Columbia University, Palisades, New York, 690 pp., 1982.
Calvo, E., Villanueva, J., Grimalt, J. O., Boelaert, A., and Labeyrie, L.: New insights into the glacial latitudinal temperature gradients in the North Atlantic. Results from Uk37' sea surface temperatures and terrigenous inputs, Earth Planet. Sc. Lett., 188, 509–519, 2001.
Calvo, E., Pelejero, C., and Logan, G. A.: Pressurized liquid extraction of selected molecular biomarkers in deep sea sediments used as proxies in paleoceanography, J. Chromatogr. A, 989, 197–205, 2003.
Chaisson, W. P., Poli, M. S., and Thunell, R. C.: Gulf Stream and Western Boundary Undercurrent variations during MIS 10–12 at Site 1056, Blake-Bahama Outer Ridge, Mar. Geol., 189, 79–105, 2002.
Channell, J. E. T., Kanamatsu, T., Sato, T., Stein, R., Alvarez Zarikian, C. A., Malone, M. J., and the.Expedition.303/306.Scientists: Proceedings IODP, 303/306, Integrated Ocean Drilling Program Management International, Inc., College Station TX, 2006.
Chapman, M. R. and Maslin, M. A.: Low-latitude forcing of meridional temperature and salinity gradients in the subpolar North Atlantic and the growth of glacial ice sheets, Geology, 27, 875–878, 1999.
Cléroux, C., Cortijo, E., Duplessy, J.-C., and Zahn, R.: Deep-dwelling foraminifera as thermocline temperature recorders, Geochem. Geophy. Geosy., 8, Q04N11, doi:10.1029/2006GC001474, 2007.
de Abreu, L., Shackleton, N. J., Schoenfeld, J., Hall, M., and Chapman, M.: Millennial-scale oceanic climate variability off the Western Iberian margin during the last two glacial periods, Mar. Geol., 196, 1–20, 2003.
de Abreu, L., Abrantes, F. F., Shackleton, N. J., Tzedakis, P. C., McManus, J. F., Oppo, D. W., and Hall, M. A.: Ocean climate variability in the eastern North Atlantic during interglacial marine isotope stage 11: A partial analogue to the Holocene?, Paleoceanography, 20, PA3009, doi:10.1029/2004PA001091, 2005.
Desprat, S., Sanchez Goni, M. F., Turon, J. L., McManus, J. F., Loutre, M. F., Duprat, J., Malaize, B., Peyron, O., and Peypouquet, J. P.: Is vegetation responsible for glacial inception during periods of muted insolation changes?, Quaternary Sci. Rev., 24, 1361–1374, 2005.

Desprat, S., Sánchez Goñi, M. F., McManus, J. F., Duprat, J., and Cortijo, E.: Millennial-scale climatic variability between 340 000 and 270 000 years ago in SW Europe: evidence from a NW Iberian margin pollen sequence, Clim. Past, 5, 53–72, 2009, http://www.clim-past.net/5/53/2009/.

Deuser, W. G. and Ross, E. H.: Seasonally Abundant Planktonic-Foraminifera of the Sargasso Sea – Succession, Deep-Water Fluxes, Isotopic Compositions, and Paleoceanographic Implications, J. Foramin. Res., 19, 268–293, 1989.

Dickson, A. J., Leng, M. J., and Maslin, M. A.: Mid-depth South Atlantic Ocean circulation and chemical stratification during MIS 10 to 12: implications for atmospheric CO_2, Clim. Past, 4, 333–344, 2008, http://www.clim-past.net/4/333/2008/.

Droxler, A. W., Alley, R. B., Howard, W. R., Poore, R. Z., and Burckle, L. H.: Introduction: Unique and Exceptionally Long Interglacial Marine Isotope Stage 11: Window into Earth Warm Future Climate, in: Earth's Climate and Orbital Eccentricity: The Marine Isotope Stage 11 Question, edited by: Droxler, A. W., Poore, R. Z., and Burckle, L. H., Geophysical Monograph, American Geophysical Union, Washington, D.C., 1–14, 2003.

EPICA Members: Eight glacial cycles from an Antarctic ice core, Nature, 429, 623–628, 2004.

Fairbanks, R. G., Wiebe, P. H., and Be, A. W. H.: Vertical-Distribution and Isotopic Composition of Living Planktonic-Foraminifera in the Western North-Atlantic, Science, 207, 61–63, 1980.

Fiúza, A. F. G.: Hidrologia e Dinamica das Aguas Costeiras de Portugal, Faculdade de Ciências da Universidade de Lisboa, Universidade de Lisboa, Lisbon, 294 pp., 1984.

Flores, J. A., Marino, M., Sierro, F. J., Hodell, D. A., and Charles, C. D.: Calcareous plankton dissolution pattern and coccolithophore assemblages during the last 600 kyr at ODP Site 1089 (Cape Basin, South Atlantic): paleoceanographic implications, Palaeogeography, Palaeoclimatology, Palaeoecology, 196, 409–426, 2003.

Flower, B. P., Oppo, D. W., McManus, J. F., Venz, K. A., Hodell, D. A., and Cullen, J. L.: North Atlantic intermediate to deep water circulation and chemical stratification during the past 1 Myr, Paleoceanography, 15, 388–403, 2000.

Fratantoni, D. M.: North Atlantic surface circulation during the 1990's observed with satellite-tracked drifters, J. Geophys. Res., 106, 22067–22093, 2001.

Guo, Z. T., Biscaye, P., Wei, L. Y., Chen, X. F., Peng, S. Z., and Liu, T. S.: Summer monsoon variations over the last 1.2 Ma from the weathering of loess-soil sequences in China, Geophys. Res. Lett., 27, 1751–1754, 2000.

Hall, I. R. and Becker, J.: Deep Western Boundary Current variability in the subtropical northwest Atlantic Ocean during marine isotope stages 12–10, Geochem. Geophy. Geosy., 8, Q06013, doi:10.1029/2006GC001518, 2007.

Hefter, J.: Analysis of Alkenone Unsaturation Indices with Fast Gas Chromatography/Time-of-Flight Mass Spectrometry, Anal. Chem., 80, 2161–2170, 2008.

Helmke, J. P. and Bauch, H. A.: Comparison of glacial and interglacial conditions between the polar and subpolar North Atlantic region over the last five climatic cycles, Paleoceanography, 18, no. 2, 1036, doi:10.1029/2002PA000794, 2003.

Helmke, J. P., Bauch, H. A., Röhl, U., and Kandiano, E. S.: Uniform climate development between the subtropical and subpolar Northeast Atlantic across marine isotope stage 11, Clim. Past, 4, 181–190, 2008, http://www.clim-past.net/4/181/2008/.

Hemming, S. R.: Heinrich events: Massive late Pleistocene detritus layers of the North Atlantic and their global climate imprint, Rev. Geophys., 42, 1–43, doi:10.1029/2003RG000128, 2004.

Hodell, D. A., Charles, C. D., and Ninnemann, U. S.: Comparison of interglacial stages in the South Atlantic sector of the southern ocean for the past 450 kyr: implifications for Marine Isotope Stage (MIS) 11, Global Planet. Change, 24, 7–26, doi:10.1016/S0921-8181(99)00069-7, 2000.

Hodell, D. A., Kanfoush, S. L., Venz, K. A., Charles, C. D., and Sierro, F. J.: The Mid-Brunhes Transition in ODP Sites 1089 and 1090 (Subantarctic South Atlantic), in: Earth's Climate and orbital eccentricity: The Marine Isotope Stage 11 Question, edited by: Droxler, A. W., Poore, R. Z., and Burckle, L. H., Geophysical Monograph, American Geophysical Union, Washington, D.C., 113–130, 2003.

Hodell, D. A., Channell, J. E. T., Curtis, J. H., Romero, O. E., and Röhl, U.: Onset of 'Hudson Strait' Heinrich Events in the Eastern North Atlantic at the end of the Middle Pleistocene Transition (~640 ka)?, Paleoceanography, 23, PA4218, doi:10.1029/2008PA001591, 2008.

Jansen, J. H. F., Kuijpers, A., and Troelstra, S. R.: A Mid-Brunhes Climatic Event: Long-Term Changes in Global Atmosphere and Ocean Circulation, Science, 232, 619–622, doi:10.1126/science.232.4750.619, 1986.

Ji, J., Ge, Y., Balsam, W., Damuth, J. E., and Chen, J.: Rapid identification of dolomite using a Fourier Transform Infrared Spectrophotometer (FTIR): A fast method for identifying Heinrich events in IODP Site U1308, Mar. Geol., 258, 60–68, 2009.

Jouzel, J., Masson-Delmotte, V., Cattani, O., Dreyfus, G., Falourd, S., Hoffmann, G., Minster, B., Nouet, J., Barnola, J. M., Chappellaz, J., Fischer, H., Gallet, J. C., Johnsen, S., Leuenberger, M., Loulergue, L., Luethi, D., Oerter, H., Parrenin, F., Raisbeck, G., Raynaud, D., Schilt, A., Schwander, J., Selmo, E., Souchez, R., Spahni, R., Stauffer, B., Steffensen, J. P., Stenni, B., Stocker, T. F., Tison, J. L., Werner, M., and Wolff, E. W.: Orbital and Millennial Antarctic Climate Variability over the Past 800,000 Years, Science, 317, 793–796, doi:10.1126/science.1141038, 2007.

Kandiano, E. S. and Bauch, H. A.: Surface ocean temperatures in the north-east Atlantic during the last 500,000 years: evidence from foraminiferal census data, Terra Nova, 15, 265–271, 2003.

Kandiano, E. S. and Bauch, H. A.: Phase relationship and surface water mass change in the Northeast Atlantic during Marine Isotope Stage 11 (MIS 11), Quaternary Res., 68, 445–455, 2007.

Knies, J., Matthiessen, J., Mackensen, A., Stein, R., Vogt, C., Frederichs, T., and Nam Il, S.: Effects of Arctic freshwater forcing on thermohaline circulation during the Pleistocene, Geology, 35, 1075–1078, 2007.

Labeyrie, L. D. and Duplessy, J. C.: Changes in the oceanic $^{13}C/^{12}C$ ratio during the last 140,000 years: High-latitude surface water records, Palaeogeogr. Palaeocl., 50, 217–240, 1985.

Lambert, F., Delmonte, B., Petit, J. R., Bigler, M., Kaufmann, P. R., Hutterli, M. A., Stocker, T. F., Ruth, U., Steffensen, J. P., and Maggi, V.: Dust-climate couplings over the past 800,000 years from the EPICA Dome C ice core, Nature, 452, 616–619, 2008.

Laskar, J., Robutel, P., Joutel, F., Gastineau, M., Correia, A. C. M., and Levrard, B.: A long-term numerical solution for the insolation quantities of the Earth, Astron. Astrophys., 428, 261–285, doi:210.1051/0004-6361:20041335, 2004.

Lea, D. W., Pak, D. K., and Spero, H. J.: Sea Surface Temperatures in the Western Equatorial Pacific During Marine Isotope Stage 11, in: Earth's Climate and orbital eccentricity: The Marine Isotope Stage 11 Question, edited by: Droxler, A. W., Poore, R. Z., and Burckle, L. H., Geophysical Monograph, American Geophysical Union, Washington, D.C., 147–156, 2003.

Levy, M., Lehahn, Y., André , J. M., Mémery, L., Loisel, H., and Heifetz, E.: Production regimes in the northeast Atlantic: A study based on Sea-viewing Wide Field-of-view Sensor (SeaWiFS) chlorophyll and ocean general circulation model mixed layer depth, J. Geophys. Res.,

110, C07S10, doi:10.1029/2004JC002771, 2005.
Lisiecki, L. E. and Raymo, M.: A Pliocene-Pleistocene stack of 57 globally distributed benthic $\delta^{18}O$ records, Paleoceanography, 20, PA1003, doi:10.1029/2004PA001071, 2005.
Loulergue, L., Schilt, A., Spahni, R., Masson-Delmotte, V., Blunier, T., Lemieux, B., Barnola, J. M., Raynaud, D., Stocker, T. F., and Chappellaz, J.: Orbital and millennial-scale features of atmospheric CH_4 over the past 800,000[thinsp]years, Nature, 453, 383–386, 2008.
Loutre, M. F. and Berger, A.: Marine Isotope Stage 11 as an analogue for the present interglacial, Global Planet. Change, 36, 209–217, 2003.
Lüthi, D., Le Floch, M., Bereiter, B., Blunier, T., Barnola, J. M., Siegenthaler, U., Raynaud, D., Jouzel, J., Fischer, H., Kawamura, K., and Stocker, T. F.: High-resolution carbon dioxide concentration record 650,000–800,000 years before present, Nature, 453, 379–382, 2008.
Martrat, B., Grimalt, J. O., Shackleton, N. J., de Abreu, L., Hutterli, M. A., and Stocker, T. F.: Four Climate Cycles of Recurring Deep and Surface Water Destabilizations on the Iberian Margin, Science, 317, 502–507, doi:10.1126/science.1139994, 2007.
McCartney, M. S. and Talley, L. D.: The Subpolar Mode Water of the North Atlantic Ocean, J. Phys. Oceanogr., 12, 1169–1188, 1982.
McManus, J., Oppo, D. W., and Cullen, J. L.: A 0.5-million-year record of millennial-scale climate variability in the North Atlantic, Science, 283, 971–975, 1999.
McManus, J., Oppo, D., Cullen, J., and Healey, S.: Marine Isotope Stage 11 (MIS 11): Analog for Holocene and Future Climate?, in: Earth's Climate and orbital eccentricity: The Marine Isotope Stage 11 Question, edited by: Droxler, A. W., Poore, R. Z., and Burckle, L. H., Geophysical Monograph, American Geophysical Union, Washington, D.C., 69–86, 2003.
Müller, P. J., Kirst, G., Ruhland, G., von Storch, I., and Rosell-Melé, A.: Calibration of the alkenone paleotemperature index Uk37' based on core-tops from the eastern South Atlantic and the global ocean (60° N-60° S), Geochim. Cosmochim. Acta, 62, 1757–1772, 1998.
Oppo, D. W., McManus, J., and Cullen, J. C.: Abrupt climate change events 500,000 to 340,000 years ago: Evidence from subpolar North Atlantic sediments, Science, 279, 1335–1338, 1998.
Oppo, D. W., Keigwin, L. D., McManus, J. F., and Cullen, J. L.: Persistent suborbital climate variability in marine isotope stage 5 and Termination II, Paleoceanography, 16, 280–292, 2001.
Ortiz, J. D., Mix, A. C., Rugh, W., Watkins, J. M., and Collier, R. W.: Deep-dwelling planktonic foraminifera of the northeastern Pacific Ocean reveal environmental control of oxygen and

carbon isotopic disequilibria, Geochim. Cosmochim. Acta, 60, 4509–4523, 1996.
Ottens, J. J.: Planktic foraminifera as North Atlantic water mass indicators, Oceanologica Acta, 14, 123–140, 1991.
Peliz, A., Dubert, J., Santos, A. M. P., Oliveira, P. B., and Le Cann, B.: Winter upper ocean circulation in the Western Iberian Basin – Fronts, Eddies and Poleward Flows: an overview, Deep Sea Research Part I: Oceanographic Research Papers, 52, 621–646, 2005.
Petit, J. R., Jouzel, J., Raynaud, D., Barkov, N. I., Barnola, J. M., Basile, I., Bender, M., Chappellaz, J., Davis, M., Delaygue, G., Delmotte, M., Kotlyakov, V. M., Legrand, M., Lipenkov, V. Y., Lorius, C., Pépin, L., Ritz, C., Saltzman, E., and Stievenard, M.: Climate and atmospheric history of the past 420,000 years from the Vostok ice core, Antarctica, Nature, 399, 429–436, 1999.
Pflaumann, U., Sarnthein, M., Chapman, M., d'Abreu, L., Funnell, B., Huels, M., Kiefer, T., Maslin, M., Schulz, H., Swallow, J., Kreveld, S. V., Vautravers, M., Vogelsang, E., and Weinelt, M.: Glacial North Atlantic: Sea-surface conditions reconstructed by GLAMAP 2000, Paleoceanography, 18, 10-11–10-28, doi:10.1029/2002PA000774, 2003.
Pierre, C., Belanger, P., Saliège, J. F., Urrutiaguer, M. J., and Murat, A.: Paleoceanography of the western Mediterranean during the Pleistocene: oxygen and carbon isotope records at Site 975, in: Proceedings ODP, Scientific Results, edited by: Zahn, R., Comas, M. C., and Klaus, A., Ocean Drilling Program, College Station, TX, 481–488, 1999.
Poli, M. S., Thunell, R. C., and Rio, D.: Millennial-scale changes in North Atlantic Deep Water circulation during marine isotope stages 11 and 12: Linkage to Antarctic climate, Geology, 28, 807–810, 2000.
Prokopenko, A. A., Williams, D. F., Kuzmin, M. I., Karabanov, E. B., Khursevich, G. K., and Peck, J. A.: Muted climate variations in continental Siberia during the mid-Pleistocene epoch, Nature, 418, 65–68, 2002.
Raffi, I., Backman, J., Fornaciari, E., Palike, H., Rio, D., Lourens, L., and Hilgen, F.: A review of calcareous nannofossil astrobiochronology encompassing the past 25 million years, Quaternary Sci. Rev., 25, 3113–3137, 2006.
Reverdin, G., Niiler, P. P., and Valdimarsson, H.: North Atlantic Ocean surface currents, J. Geophy. Res., 108(C1), 3002, doi:10.1029/2001JC001020, 2003.
Rickaby, R. E. M., and Elderfield, H.: Evidence from the high-latitude North Atlantic for variations in Antarctic Intermediate water flow during the last deglaciation, Geochem. Geophy. Geosy., 6, 1–12, 2005.

Rios, A. F., Perez, F. F., and Fraga, F.: Water Masses in the Upper and Middle North-Atlantic Ocean East of the Azores, Deep-Sea Res. I, 39, 645–658, 1992.
Rodrigues, T., Voelker, A. H. L., Grimalt, J., and Abrantes, F.: Millennial-scale variability in marine and terrestrial climate records off Portugal during MIS 9–15, in preperation.
Ruddiman, W. F.: Late Quaternary deposition of ice-rafted sand in the subpolar North Atlantic (lat 40° to 65°N), Geol. Soc. Am. Bull., 88, 1813–1827, 1977.
Ruddiman, W. F.: Orbital changes and climate, Quaternary Sci. Rev., 25, 3092–3112, 2006.
Salgueiro, E., Voelker, A., Abrantes, F., Meggers, H., Pflaumann, U., Loncaric, N., Gonzalez-Alvarez, R., Oliveira, P., Bartels-Jonsdottir, H. B., Moreno, J., and Wefer, G.: Planktonic foraminifera from modern sediments reflect upwelling patterns off Iberia: Insights from a regional transfer function, Mar. Micropaleontol., 66, 135–164, doi:10.1016/j.marmicro.2007.09.003, 2008.
Shackleton, N. J.: The last interglacial in the marine and terrestrial records, Proceedings of the Royal Society of London, 6, 183–190, 1969.
Shackleton, N. J.: Attainment of isotopic equilibrium between ocean water and the benthonic foraminifera genus Uvigerina: Isotopic changes in the ocean during the last Glacial, Colloques Internationaux du C. N. R. S., 219, 203–209, 1974.
Shackleton, N. J., Hall, M. A., and Vincent, E.: Phase relationships between millennial-scale events 64,000–24,000 years ago, Paleoceanography, 15, 565–569, 2000.
Siegenthaler, U., Stocker, T. F., Monnin, E., Luthi, D., Schwander, J., Stauffer, B., Raynaud, D., Barnola, J. M., Fischer, H., Masson-Delmotte, V., and Jouzel, J.: Stable Carbon Cycle-Climate Relationship During the Late Pleistocene, Science, 310, 1313–1317, 2005.
Spahni, R., Chappellaz, J., Stocker, T. F., Loulergue, L., Hausammann, G., Kawamura, K., Flückiger, J., Schwander, J., Raynaud, D., Masson-Delmotte, V., and Jouzel, J.: Atmospheric Methane and Nitrous Oxide of the Late Pleistocene from Antarctic Ice Cores, Science, 310, 1317–1321, 2005.
Stein, R., Hefter, J., Grützner, J., Voelker, A., and Naafs, B. D. A.: Variability of surface-water characteristics and Heinrich-like Events in the Pleistocene mid-latitude North Atlantic Ocean: Biomarker and XRD records from IODP Site U1313 (MIS 16–9), Paleoceanography, 24, PA2203, doi:10.1029/2008PA001639, 2009.
Stirling, C. H., Esat, T. M., Lambeck, K., McCulloch, M. T., Blake, S. G., Lee, D. C., and Halliday, A. N.: Orbital Forcing of the Marine Isotope Stage 9 Interglacial, Science, 291, 290–293, 2001.

Tzedakis, P. C., Andrieu, V., de Beaulieu, J. L., Crowhurst, S., Follieri, M., Hooghiemstra, H., Magri, D., Reille, M., Sadori, L., Shackleton, N. J., and Wijmstra, T. A.: Comparison of terrestrial and marine records of changing climate of the last 500,000 years, Earth Planet. Sci. Lett., 150, 171–176, 1997.

Tzedakis, P. C., Roucoux, K. H., de Abreu, L., and Shackleton, N. J.: The Duration of Forest Stages in Southern Europe and Interglacial Climate Variability, Science, 306, 2231–2235, 2004.

Tzedakis, P. C., Hooghiemstra, H., and Palike, H.: The last 1.35 million years at Tenaghi Philippon: revised chronostratigraphy and long-term vegetation trends, Quaternary Sci. Rev., 25, 3416–3430, 2006.

Tzedakis, P. C., Pälike, H., Roucoux, K. H., and de Abreu, L.: Atmospheric methane, southern European vegetation and low-mid latitude links on orbital and millennial timescales, Earth Planet. Sci. Lett., 277, 307–317, 2009.

van Aken, H. M.: The hydrography of the mid-latitude Northeast Atlantic Ocean – Part III: the subducted thermocline water mass, Deep-Sea Res. I, 48, 237–267, 2001.

Venz, K. A., Hodell, D. A., Stanton, C., and Warnke, D. A.: A 1.0 Myr record of Glacial North Atlantic Intermediate Water variability from ODP site 982 in the northeast Atlantic, Paleoceanography, 14, 42–52, 1999.

Villanueva, J., Grimalt, J. O., Cortijo, E., Vidal, L., and Labeyrie, L.: A biomarker approach to the organic matter deposited in the North Atlantic during the last climatic cycle, Geochim. Cosmochim. Acta, 61, 4633–4646, 1997.

Voelker, A., Martin, P., Lebreiro, S., and Abrantes, F.: Millennial-scale Deep/Intermediate Water Changes at the Mid-depth Portuguese Margin During Marine Isotope Stage (MIS) 11, Quaternary International, 167–168, 436, 2007.

Voelker, A. H. L.: Zur Deutung der Dansgaard-Oeschger Ereignisse in ultra-hochauflösenden Sedimentprofilen aus dem Europäischen Nordmeer, DSc dissertation, Berichte-Reports, Institut für Geowissenschaften, Universität Kiel, no. 9, University of Kiel, Kiel, Germany, 278 pp., 1999.

Voelker, A. H. L., Grützner, J., and Hodell, D. A.: High-frequency Changes in Surface and Deep Water Hydrography in the Mid-latitude North Atlantic during Marine Isotope Stages 11–15: New Insights from IODP Sites U1313 and U1308, Geochem. Geophy. Geosy., in revision, 2009.

von Grafenstein, R., Zahn, R., Tiedemann, R., and Murat, A.: Planktonic δ^{18}O records at Sites

976 and 977, Alboran Sea: Stratigraphy, forcing, and paleoceanographic implications, in: Proceedings ODP, Scientific Results, edited by: Zahn, R., Comas, M. C., and Klaus, A., Ocean Drilling Program, College Station, TX, 469–479, 1999.

Watanabe, O., Jouzel, J., Johnsen, S., Parrenin, F., Shoji, H., and Yoshida, N.: Homogeneous climate variability across East Antarctica over the past three glacial cycles, Nature, 422, 509–512, 2003.

Weirauch, D., Billups, K., and Martin P.: Evolution of Millennial-Scale Climate Variability During the Mid Pleistocene, Paleoceanography, 23, PA 3216, doi:10.1029/2007PA001584, 2008.

Table 1. Locations of core sites and their respective hydrographic and productivity regimes.

Site	Latitude	Longitude	Water depth	Surface water sources	Productivity regime
ODP site 980	55°29.09′ N	14°42.13′ W	2168 m	Rockall Trough branch of North Atlantic Current	Subpolar regime
IODP site U1313	41°00.07′ N	32°57.40′ W	3412 m	North Atlantic Current derived waters	Transitional zone between subpolar and mid-latitude regimes
MD01-2446	39°03.35′ N	12°37.44′ W	3570 m	Portugal Current	Mid-latitude regime
MD03-2669	39°02.20′ N	10°39.63′ W	1895 m	Upwelling and Iberian Poleward Current	Seasonal upwelling
MD01-2443	37°52.89′ N	10°10.57′ W	2941 m	Upwelling and Iberian Poleward Current	Seasonal upwelling
ODP site 1056	32°29.10′ N	76°19.80′ W	2167 m	Gulf Stream	Subtropical regime
ODP site 1058	31°41.40′ N	75°25.80′ W	2985 m		

CPD
5, 1553–1607, 2009

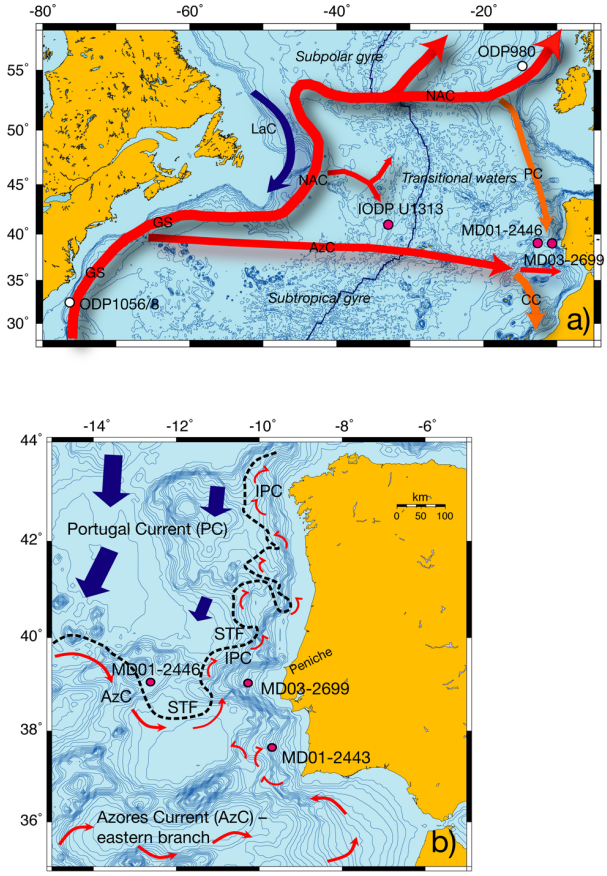

Fig. 1. **(a)** Core locations and major surface water currents in the North Atlantic (Fratantoni, 2001): GS = Gulf Stream; NAC = North Atlantic Current; AzC = Azores Current; CC = Canary Current; PC = Portugal Current; LaC = Labrador Current. **(b)** Winter circulation scheme off Portugal after (Peliz et al., 2005) with IPC = Iberian Poleward Current and STF = Subtropical front.

CC BY

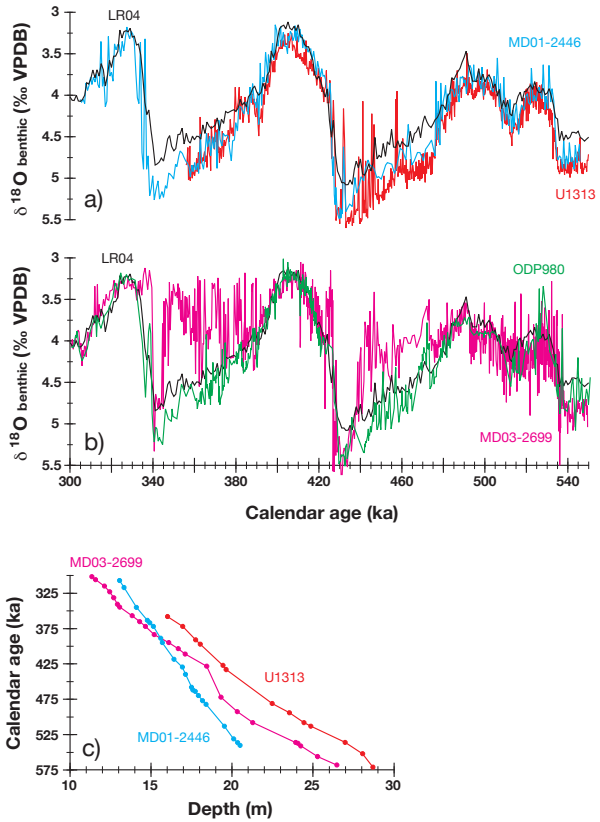

Fig. 2. **(a)** Benthic δ^{18}O records of IODP site U1313 (red) and MD01-2446 (cyan) in comparison to the LR04 stack (black) (Lisiecki and Raymo, 2005); **(b)** Benthic δ^{18}O record of MD03-2699 (magenta) in comparison to ODP site 980 (green; on LR04 timescale) and the LR04 stack (black). **(c)** Age-depth relationships for IODP site U1313, MD01-2446 and MD03-2699.

CPD
5, 1553–1607, 2009

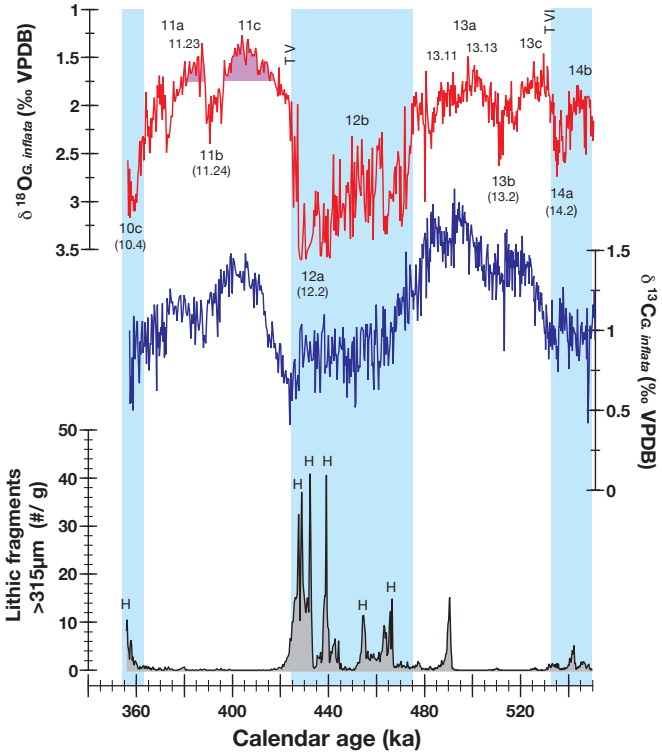

Fig. 3. Surface water records for IODP site U1313 in the mid-latitude North Atlantic. From top to bottom: *G. inflata* δ^{18}O (‰VPDB), *G. inflata* δ^{13}C (‰VPDB), and lithics concentration (#/g). Blue bars mark glacial MIS 10, 12 and 14. Substages (e.g. 11c) are indicated above and below the δ^{18}O record as well as some isotopic events (e.g. 10.4). T IV, V and VI refer to Terminations VI, V and VI. H indicates IRD peaks with Heinrich-type signatures (Stein et al., 2009).

CPD
5, 1553–1607, 2009

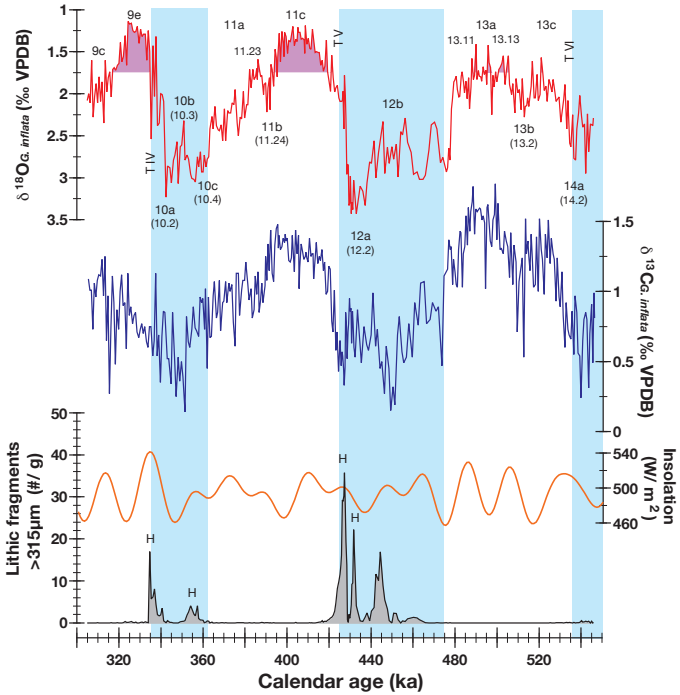

Fig. 4. Surface water records for core MD01-2446, the offshore site off Portugal. From top to bottom: *G. inflata* δ^{18}O (‰VPDB), *G. inflata* δ^{13}C (‰VPDB), June 21st insolation at 65° N (Laskar et al., 2004), and lithics concentration (#/g). Blue bars mark glacial MIS 10, 12 and 14. Substages (e.g. 11c) are indicated above and below the δ^{18}O record as well as some isotopic events (e.g. 10.4). T IV, V and VI refer to Terminations VI, V and VI. H indicates Heinrich-type ice-rafting events.

CPD
5, 1553–1607, 2009

CC BY

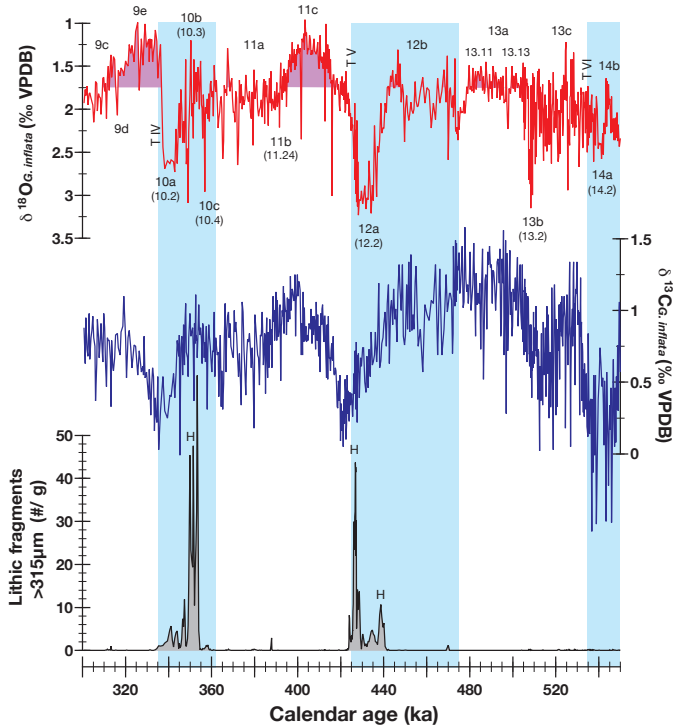

Fig. 5. Surface water records for core MD03-2699, the nearshore site off Portugal. From top to bottom: *G. inflata* δ^{18}O (‰VPDB), *G. inflata* δ^{13}C (‰VPDB), and lithics concentration (#/g). Blue bars mark glacial MIS 10, 12 and 14. Substages (e.g. 11c) are indicated above and below the δ^{18}O record as well as some isotopic events (e.g. 10.4). T IV, V and VI refer to Terminations VI, V and VI. H indicates Heinrich-type ice-rafting events.

CPD
5, 1553–1607, 2009

CC BY

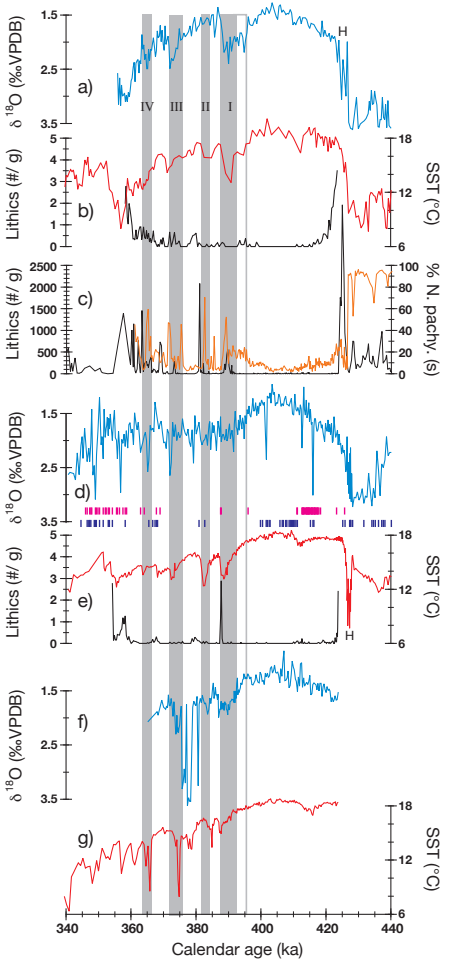

Fig. 6.

CPD
5, 1553–1607, 2009

CC BY

Fig. 6. Close-ups of MIS 11 in the records of IODP Site U1313 **(a, b)**, ODP Site 980 **(c)**, MD03-2699 **(d, e)** and southern Portuguese site MD01-2443 **(f, g)**; (de Abreu et al., 2005; Martrat et al., 2007).*G. inflata* δ^{18}O records are shown in blue (a, d, f), alkenone-based mean annual sea surface temperature (SST) records in red (b, e, g). The abundance of Lithics >315 μm (black; only sections with <4 grains/g) are shown for IODP Site U1313 (b) and core MD03-2699 (e) and >150 μm for ODP Site 980 (c; Oppo et al., 1998). Panel (c) also includes the % *N. pachyderma* (s) record of ODP Site 980 (orange; Oppo et al. 1998). In panel (d) magenta bars indicate presence of *Globorotalia menardii* and dark blue ones of Sphaeroidinella dehiscens in the respective levels. MD01-2443 data is shown using the age model of (Tzedakis et al., 2009) that links the MD01-2443 benthic δ^{18}O data to the EDC δD record on the EDC 3 timescale (Jouzel et al., 2007) following the approach of (Shackleton et al., 2000). Grey bars indicate stadials (numbered I to IV) within MIS 11a. The bar outlined in grey during the oldest stadial marks the interval when cold conditions already prevailed at (I)ODP Sites U1313 and 980. H denotes the Heinrich-type ice-rafting event associated with Termination V.

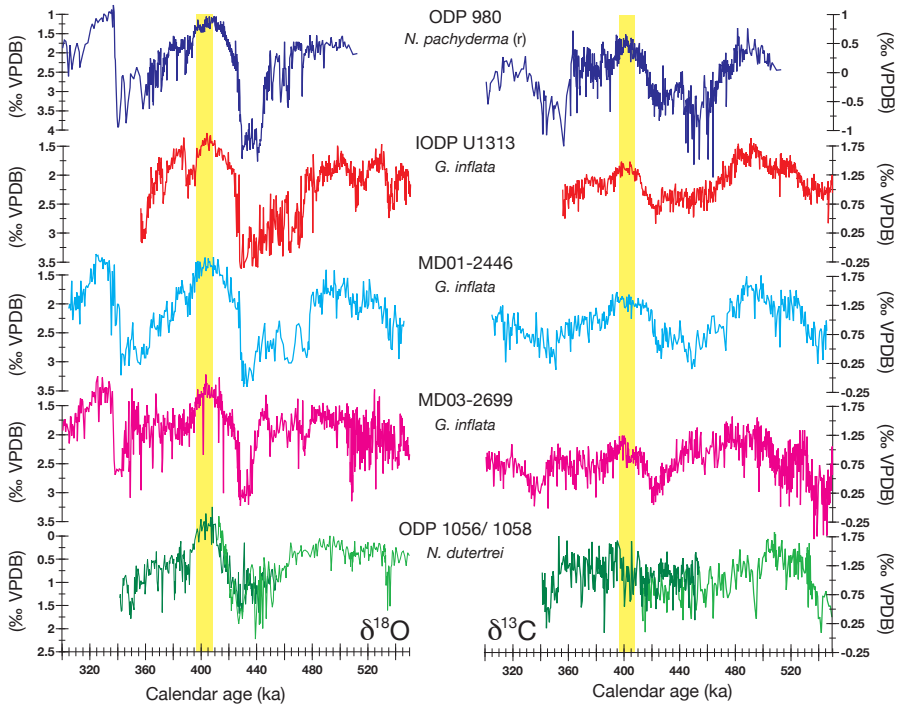

Fig. 7. North Atlantic planktonic foraminifer stable isotope records with δ^{18}O records on the left and δ^{13}C records on the right. Sites are arranged from North to South: ODP Site 980 (dark blue), IODP Site U1313 (red), MD01-2446 (light blue), MD03-2699 (magenta), and ODP Sites 1056 (dark green) and 1058 (light green) combined. Yellow bars highlight the period of the MIS 11c sea level highstand.

CPD
5, 1553–1607, 2009

CC BY

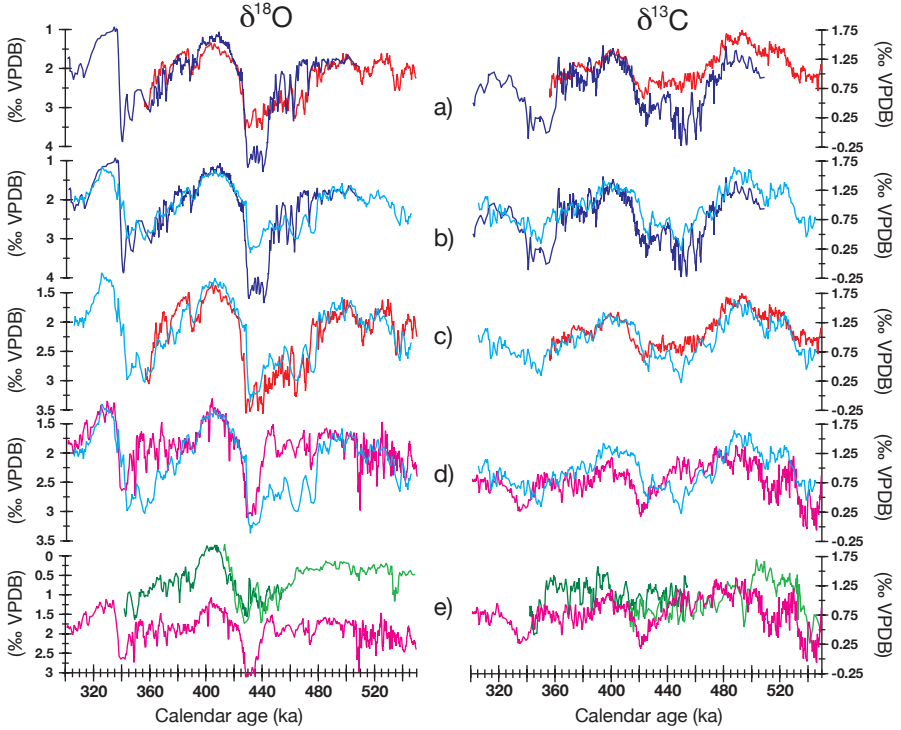

Fig. 8. Direct comparison between sites based on 3 point average records (δ^{18}O left, δ^{13}C right side). Colors for sites as in Fig. 7. **(a)** IODP Site U1313 vs. ODP Site 980. For better comparison ODP Site 980 *N. pachyderma* (r) δ^{13}C data was adjusted to dissolved inorganic carbon (DIC) by adding 0.85‰(Labeyrie and Duplessy, 1985). **(b)** MD01-2446 vs. ODP Site 980 (with δ^{13}C adjusted); **(c)** MD01-2446 vs. IODP Site U1313; **(d)** MD01-2446 vs. MD03-2699; **(e)** ODP Sites 1056 and 1058 vs. MD03-2699.

CPD
5, 1553–1607, 2009

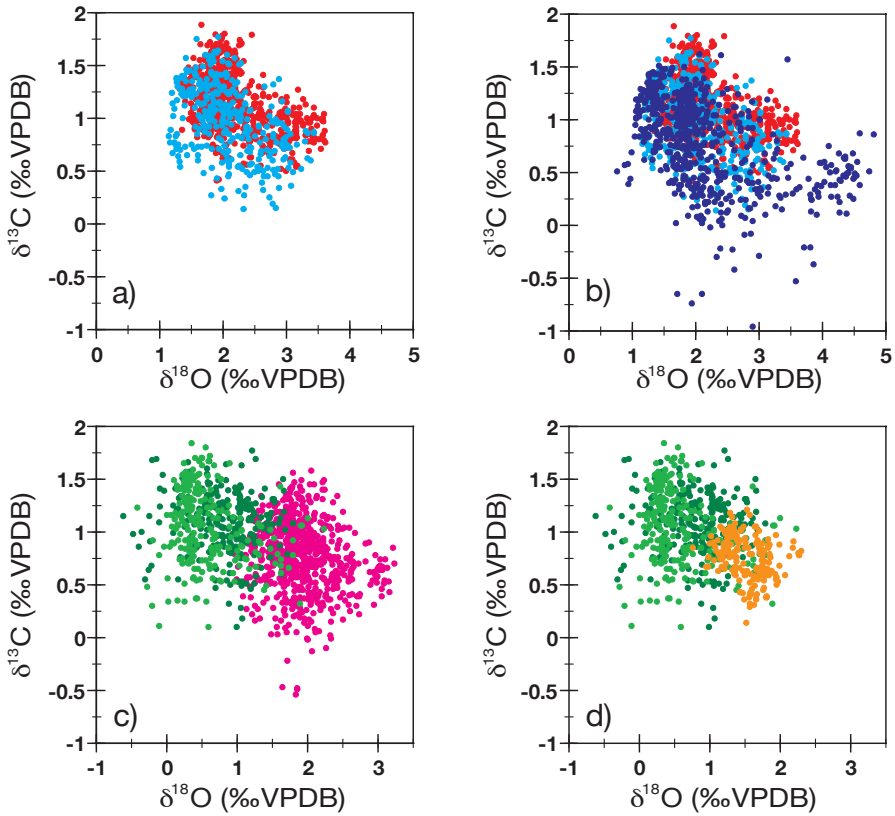

Fig. 9. $\delta^{18}O$ versus $\delta^{13}C$ scatter plots of the records shown in Fig. 7. **(a)** IODP Site U1313 (red) and MD01-2446 (light blue); **(b)** IODP Site U1313 (red), MD01-2446 (light blue), and ODP Site 980 (dark blue); **(c)** MD03-2699 (magenta) and ODP Sites 1056 (dark green) and 1058 (light green); **(d)** ODP Sites 1056 (dark green) and 1058 (light green) and MD01-2443 (orange; de Abreu et al., 2005; with extreme values between 375 and 381 ka excluded).

CPD
5, 1553–1607, 2009